Deuteron Stripping on Deformed Nuclei*

P. J. IANO
University of Pittsburgh, Pittsburgh, Pennsylvania
and
Western Reserve University, Cleveland, Ohio

AND

N. AUSTERN
University of Pittsburgh, Pittsburgh, Pennsylvania

(Received 31 May 1966)

Interference of indirect transition amplitudes with the direct transition amplitude for deuteron stripping on deformed nuclei is investigated. The indirect transitions that are considered are those that arise via intermediate rotational excitations of the target and product nuclei. These indirect transitions are introduced by generalizing the initial and final distorted waves so that they include inelastic amplitudes. A straightforward coupled-channel treatment of the generalized distorted waves is described. However, a quantitative investigation of the coupled-channel formulation is not attempted because of the enormous numerical difficulties that such a procedure would present. Instead, the rotational motion of the target is treated adiabatically; thereby, in principle, inelastic amplitudes in all rotational channels are accounted for simultaneously. Further simplification is achieved by treating the coupling of the rotational coordinates to the projectile coordinates only to first order. Calculations are performed for deuteron stripping on Mg^{24} and U^{238}. The calculations indicate that: (a) the indirect amplitudes are small; (b) the indirect amplitudes are affected more strongly by intermediate excitations in the deuteron channel than by intermediate excitations in the proton channel; (c) the indirect amplitudes generally flatten the angular distributions of the reaction protons; and (d) the ratio of the strength of the indirect transitions to that of the direct transition is fairly independent of the mass of the target. Although the spin-orbit force is neglected, the theory predicts a J dependence in the angular distributions that is significant at all angles. The indirect stripping amplitudes are small; however, they produce measurable effects in the differential cross section when they add coherently to the direct amplitude. The most dramatic effects of the indirect amplitudes are changes of the angular distributions of the reaction protons. In addition, the calculated spectroscopic coefficients are changed by a significant amount when the indirect amplitudes are taken into account.

1. INTRODUCTION

THE deuteron stripping reaction has been treated most successfully by the distorted-wave Born approximation (DWBA),[1–3] under the assumption that the transition takes place directly from the incident deuteron channel to the exit proton channel, without any intermediate step that excites internal variables of the target nucleus.

However, intermediate inelastic excitations may well play a role in the stripping process. For example, the incident deuteron might excite the target nucleus prior to the stripping event, or the emergent proton might excite the residual nucleus. Such processes would cause "indirect" contributions to the stripping amplitude and these might violate selection rules to which the direct amplitude is subject, or they might interfere to an appreciable extent with the direct amplitude in case it is allowed. The present paper is devoted to an investigation of such indirect contributions to the stripping amplitude. It is related to other recent work by Penny and Satchler,[4] Kozlowsky and de-Shalit,[5] Sorensen, Dillenburg, and Drisko,[6,7] and Levin.[8]

We treat only collective inelastic excitations of the target and residual nuclei, because these are known to be much stronger than single-particle excitations.[9,10] Also, even though the general methods of this paper are equally applicable for collective rotations or vibrations, the analysis to be given will be specialized to the treatment of rotational excitations of permanently deformed nuclei.

The inelastic excitations are treated in the same manner that is employed by Penny and Satchler[4]; namely, distorted waves that are generalized to account for inelastic scattering are introduced into the usual DWBA theory. Each such generalized distorted wave, whether in the incident or emergent channel, describes scattering of a projectile by a spheroidally deformed optical potential. Of course, eigenfunctions of deformed single-particle potentials also are used for the bound orbitals of deformed nuclei.[11] However, the effects intro-

* Work supported in part by the National Science Foundation.

[1] J. Horowitz and A. M. L. Messiah, J. Phys. Radium **14**, 695 (1953).

[2] W. Tobocman and M. H. Kalos, Phys. Rev. **97**, 132 (1955).

[3] W. Tobocman and M. H. Kalos, Phys. Rev. **115**, 99 (1959).

[4] S. K. Penny and G. R. Satchler, Nucl. Phys. **53**, 145 (1964); S. K. Penny, thesis, University of Tennessee, 1966 (unpublished).

[5] B. Kozlowsky and A. de-Shalit, Nucl. Phys. **77**, 215 (1966).

[6] Darcy Dillenburg and Raymond A. Sorensen, Bull. Am. Phys. Soc. **10**, 40 (1965).

[7] Raymond A. Sorensen, Darcy Dillenburg, and R. M. Drisko (to be published).

[8] F. S. Levin, Phys. Rev. **147**, 715 (1966).

[9] B. L. Cohen, Phys. Rev. **105**, 1549 (1957).

[10] B. L. Cohen, Phys. Rev. **116**, 426 (1959).

[11] Sven Gösta Nilsson, Kgl. Danske Videnskab. Selskab, Mat. Fys. Medd. **29**, No. 16 (1955).

duced in stripping theory by the use of such bound orbitals are accounted for fully by computing the appropriate spectroscopic coefficients, as was first done by Satchler.[12] The use of distorted waves that are affected by the nuclear deformation will now introduce additional effects.

The effects caused by using distorted waves that are affected by the deformation were first investigated by Sawicki and Satchler[13]; however, they only introduced distortion by the device of using an angle-dependent cutoff in the Butler plane-wave theory. The present article can be regarded as a generalization of the work of Sawicki and Satchler. As in their work, the collective coordinates are treated adiabatically[14,15]; thus, it is considered that during the course of the stripping event the deformed nucleus changes neither its deformation nor its orientation. Not only does this adiabatic approximation greatly simplify the calculation, but it parallels closely the physical picture of deformed bound states. Thus the present article carries on equal terms all the effects of nuclear deformation.

In Sec. 2, a formal description of the stripping process is presented. This description is used to compare the distorted-wave treatment and two models which account for indirect stripping processes.[4,5] In Sec. 3, the adiabatic approximation is discussed in relation to its application to the inelastic scattering of projectiles on deformed nuclei. In Sec. 4, the adiabatic model of stripping is developed and, in Sec. 5, the model is applied to deuteron stripping on Mg^{24} and U^{238}.

Further details of the present work may be found in Ref. 16.

2. DESCRIPTIONS OF THE STRIPPING REACTION

The theory to be presented will be cast in terms of the reaction, $A(d,p)B$; however, it is readily extended to other stripping and pickup reactions. The dynamical system consists of the neutron and proton of the incident deuteron plus the A nucleons of the target nucleus.

The Hamiltonian for this system of $A+2$ nucleons will be displayed in six parts. Assuming the target to be infinitely heavy, the Hamiltonian for the system is

$$H=h_i(\xi)+T_n+T_p+V_n+V_p+V_{np}, \qquad (2.1)$$

where h_i is the Hamiltonian of the isolated A nucleons of the target nucleus. The variable ξ represents the internal coordinates of the target. T_n is the kinetic-energy operator of the neutron motion. T_p is the kinetic-energy operator of the proton motion. V_n is the interaction of the neutron with the target nucleus. V_p is the interaction of the proton with the target nucleus. V_{np} is the interaction between the neutron and proton.

The state of motion of the system before the collision will be assumed to consist of a deuteron plane wave incident on a target nucleus in its ground state. The quantity to be calculated is the transition amplitude from the initial system to a final configuration consisting of a proton plane wave and a product nucleus in either its ground state or some low-lying excited state.

Ignoring the small exchange ("knockout") term,[17] the stripping amplitude is[18]

$$T_{dp}=(N+1)^{1/2}([\exp i\mathbf{k}_p\cdot\mathbf{r}_p]S_{\mu_p}(\sigma_p)\Psi_B(n,\xi), [V_{np}+V_p]\Psi_i^{(+)}(n,p,\xi)). \qquad (2.2)$$

The symbols n and p label the neutron and proton of the incident deuteron. The variable n represents the spin σ_n and space $\mathbf{r}_n$ coordinates of the neutron; and p represents the spin σ_p and space $\mathbf{r}_p$ coordinates of the proton. The function S_{μ_p} is the spin function of the proton, with spin projection $\hbar\mu_p$. The wave function Ψ_B represents the internal motion of the product nucleus and is antisymmetric in the neutron and proton coordinates separately. The target nucleus is assumed to contain N neutrons. The function $\Psi_i^{(+)}$ is an eigenfunction of the Hamiltonian H of the entire system, such that

$$\Psi_i^{(+)}\sim S_{\mu_d}(\sigma_n,\sigma_p)\phi_{np}(r_{np}) \times\Psi_A(\xi)\exp i\mathbf{k}_d\cdot\mathbf{r}_d+\text{outgoing waves}. \qquad (2.3)$$

The function S_{μ_d} is the spin function of the deuteron, and ϕ_{np} is the wave function of the internal motion of the deuteron. The wave function Ψ_A represents the target nucleus in its ground state and is taken antisymmetric in the neutron and proton coordinates separately.

The transition amplitude can be cast in a more symmetric form by incorporating the effects of V_p into the final-state wave function. Equation (2.2) becomes[18]

$$T=(N+1)^{1/2}(\Psi_f^{(-)}(n,p,\xi),V_{np}\Psi_i^{(+)}(n,p,\xi)), \qquad (2.4)$$

where

$$\{[h_i(\xi)+T_n+V_n]+[T_p+V_p]-E\}\Psi_f^{(-)\dagger}=0. \qquad (2.5)$$

The boundary conditions on $\Psi_f^{(-)}$ are

$$\Psi_f^{(-)}\sim S_{\mu_p}(\sigma_p)\Psi_B(n,\xi) \times\exp i\mathbf{k}_p\cdot\mathbf{r}_p+\text{incoming waves}. \qquad (2.6)$$

Most theories of the deuteron stripping reactions use Eq. (2.4) to one degree of approximation or another.

2.1. Distorted-Wave Born Approximation

The most successful theory of deuteron stripping has been the distorted-wave Born approximation.[1-3] This theory assumes that most of the amplitude of $\Psi_i^{(+)}$ is

[12] G. R. Satchler, Ann. Phys. (N.Y.) 3, 275 (1958).
[13] J. Sawicki and G. R. Satchler, Nucl. Phys. 7, 289 (1958).
[14] S. I. Drozdov, Zh. Eksperim. i Teor. Fiz. 28, 734 (1955); 28, 736 (1955) [English transls.: Soviet Phys.—JETP 1, 591 (1955); 1, 588 (1955)].
[15] J. S. Blair, Phys. Rev. 115, 928 (1959).
[16] P. J. Iano, thesis, University of Pittsburgh, 1965 (unpublished).
[17] L. S. Rodberg, Nucl. Phys. 47, 1 (1963).
[18] M. L. Goldberger and K. M. Watson, *Collision Theory* (John Wiley & Sons, Inc., New York, 1964).

in the elastic channel, and therefore approximates $\Psi_i^{(+)}$ by

$$\Psi_i^{(+)}\approx S_{\mu_d}(\sigma_n,\sigma_p)\phi_{np}(r_{np})\Psi_A(\xi)\chi_A^{(+)}(\mathbf{r}_d). \quad (2.7)$$

The wave function $\chi_A^{(+)}$ describes the elastic scattering of the deuteron in the entrance channel. Similarly, the final-state wave function is approximated as

$$\Psi_f^{(-)}\approx S_{\mu_p}(\sigma_p)\Psi_B(n,\xi)\chi_B^{(-)}(\mathbf{r}_p), \quad (2.8)$$

where $\chi_B^{(-)}$ is the elastic-scattering wave function of the proton in the exit channel. The distorted waves, $\chi_A^{(+)}$ and $\chi_B^{(-)}$, are calculated with optical-model potentials, the parameters of which are chosen to reproduce the elastic-scattering data. The transition amplitude, Eq. (2.4), becomes

$$T\approx T_0,$$

where

$$T_0=(N+1)^{1/2}(\chi_B^{(-)},\langle S_{\mu_p}\Psi_B|S_{\mu_d}\Psi_A\rangle D_{np}\chi_A^{(+)}). \quad (2.9)$$

The function D_{np} is defined as

$$D_{np}=V_{np}\phi_{np}, \quad (2.10)$$

and is usually taken to have zero range; thus, the six-dimensional integration over the spatial coordinates $\mathbf{r}_p$ and $\mathbf{r}_n$ reduces to a more manageable three-dimensional integral.

2.2. Generalized Distorted-Wave Method

The estimate of the transition amplitude can be improved by including inelastic amplitudes in the entrance and exit wave functions. At present, a straightforward application of this approach is being carried through by Penny and Satchler.[4] The wave function $\Psi_i^{(+)}$ of Eq. (2.4) is approximated by

$$\Psi_i^{(+)}\approx S_{\mu_d}\phi_{np}\sum_{A'}\Psi_{A'}(\xi)\chi_{A'}^{(+)}(\mathbf{r}_d). \quad (2.11)$$

The wave function $\Psi_i^{(+)}$ is a generalized distorted wave in that it describes not only the scattering in the entrance channel, $A'=A$, but also in the inelastic channels, $A'\neq A$. The wave functions of relative motion obey the boundary conditions

$$\chi_{A'}^{(+)}\sim\delta_{AA'}\exp i\mathbf{k}_d\cdot\mathbf{r}_d+\text{outgoing waves}. \quad (2.12)$$

Similarly, the final-state wave function of Eq. (2.4) is approximated as

$$\Psi_f^{(-)}\approx S_{\mu_p}\sum_{B'}\Psi_{B'}(n,\xi)\chi_{B'}^{(-)}(\mathbf{r}_p). \quad (2.13)$$

Here the wave functions of relative motion obey the boundary conditions

$$\chi_{B'}^{(-)}\sim\delta_{BB'}\exp i\mathbf{k}_p\cdot\mathbf{r}_p+\text{incoming waves}. \quad (2.14)$$

Both (2.11) and (2.13) assume spin-independent interactions between projectile and target.

In the entrance channel, for example, the wave functions of relative motion obey the set of simultaneous differential equations:

$$[T_d-(E-\epsilon_{A'})]\chi_{A'}^{(+)}=-\sum_{A''}\langle\Psi_{A'}(\xi)|V(\xi,\mathbf{r}_d)|\Psi_{A''}(\xi)\rangle\chi_{A''}^{(+)}, \quad (2.15)$$

where T_d is the kinetic-energy operator for the deuteron center of mass. The equations, (2.15), are made manageable by limiting the calculation to a few chosen channels, A'. All other channels are ignored. The interaction $V(\xi,\mathbf{r}_d)$ is a generalized optical potential, that describes both the elastic scattering that may take place in each of the chosen channels, and also the inelastic coupling among the channels. The detailed form of this interaction is determined by whatever model of the deuteron-nucleus interaction may seem appropriate. For example, if collective excitations of deformed nuclei should be of interest, as in the present work, then one generally uses a deformed optical potential for $V(\xi,\mathbf{r}_d)$. Equations (2.15) present a typical coupled-channel problem. They are solved by numerical integration.

The wave functions $\chi_B^{(-)}$ are handled in a similar fashion.

The transition amplitude of Eq. (2.4) becomes

$$T\approx T_{\text{c.c.}},$$

where

$$T_{\text{c.c.}}=(N+1)^{1/2}\times\sum_{A'B'}(\chi_{B'}^{(-)},\langle S_{\mu_p}\Psi_{B'}|S_{\mu_d}\Psi_{A'}\rangle D_{np}\chi_{A'}^{(+)}). \quad (2.16)$$

Again, D_{np} can be approximated to have zero range, and therefore the six-dimensional integration over $\mathbf{r}_p$ and $\mathbf{r}_n$ reduces to a three-dimensional integral.

The theory to be developed in this work will essentially be a coupled-channel theory. However, advantage will be taken of the assumption that the target and product nuclei are strongly deformed. The wave functions in the deuteron and proton channels will be calculated under an adiabatic approximation[15,16]; thus, in principle, all rotational excitations are coupled in simultaneously.

2.3. Core-Excitation Model

There is a variant method in use to account for inelastic excitations in the exit channel. Kozlowsky and de-Shalit[5] call it the "core-excitation model." Work on this method is also being carried out by Sorensen, Dillenburg, and Drisko[6,7]; and by Levin.[8]

The proton interaction V_p is divided as

$$V_p=V_p^0+V_p^c. \quad (2.17)$$

The first term V_p^0 is taken to be just the optical potential that describes the elastic scattering of the protons, therefore the remaining term V_p^c is the part of the proton interaction which couples inelastic states to the proton elastic channel. The transition amplitude now takes the form

$$T=(N+1)^{1/2}(\Psi_B(n,\xi)S_{\mu_p}(\sigma_p)\chi_B^{(-)}(\mathbf{r}_p),\ [V_p^c+V_{np}]\Psi_i^{(+)}(n,p,\xi)). \quad (2.18)$$

This expression is exact as it stands. For computational purposes, however, $\Psi_i^{(+)}$ is replaced by the distorted-wave Born approximation, Eq. (2.7). The transition amplitude then becomes

$$T \approx T_0 + T_p,$$

where

$$T_p = (N+1)^{1/2} \times (\chi_B^{(-)}, \langle S_{\mu_p}\Psi_B | V_p^c | S_{\mu_d}\Psi_A\rangle \phi_{np}\chi_A^{(+)}). \quad (2.19)$$

The amplitude T_0 is given by Eq. (2.9). Because the initial-state wave function in Eq. (2.18) is replaced by an elastic-scattering wave function contributions to the transition amplitude from inelastic deuteron channels are not accounted for.

The amplitude T_0 is the usual distorted-wave amplitude. The additional amplitude T_p is more difficult to handle than T_0. The computation of T_0 is simplified due to the short range of D_{np}; however it is clear that an accurate calculation of T_p would require a finite-range treatment of the spatial coordinates.

3. ADIABATIC APPROXIMATION

In this section, the scattering of projectiles by deformed nuclei will be discussed. The rotational motion of the deformed nucleus will be treated adiabatically and a first-order perturbation theory will be developed in the context of the adiabatic approximation.

3.1. Adiabatic Approximation

The subject of discussion is an approximation procedure for calculating the wave function that describes the scattering of a projectile by a spheroidal rotator. The Hamiltonian for the system is

$$H = h(\theta) + [T + V(\theta,\mathbf{r})], \quad (3.1)$$

where $h(\theta)$ is the Hamiltonian of the rotator. T is the kinetic-energy operator of the projectile. $V(\theta,\mathbf{r})$ is the deformed optical well which represents the interaction between the projectile and the rotator. The intrinsic nuclear coordinates are not displayed explicitly in Eq. (3.1), since the model ignores excitations of the intrinsic structure.

The Schrödinger equation for the scattering wave function is

$$(H-E)\Psi^{(+)}(\theta,\mathbf{r}) = 0. \quad (3.2)$$

The boundary conditions on $\Psi^{(+)}$ are

$$\Psi^{(+)} \sim \Psi_0(\theta)\, \exp i\mathbf{k}\cdot\mathbf{r} + \text{outgoing waves}, \quad (3.3)$$

where Ψ_0 is the rotator wave function in the entrance channel. It obeys the following Schrödinger equation.

$$[h(\theta) - \epsilon_0]\Psi_0(\theta) = 0. \quad (3.4)$$

In most cases of physical interest, Ψ_0 is the ground-state rotator wave function.

The adiabatic approximation is an approximation of the wave equation, Eq. (3.2). Substitution of (3.1) into (3.2) yields

$$[h(\theta) + T + V(\theta,\mathbf{r})]\Psi^{(+)}(\theta,\mathbf{r}) = E\Psi^{(+)}(\theta,\mathbf{r}). \quad (3.5)$$

This equation is rewritten in a slightly different form.

$$(\epsilon_0 + T + V)\Psi^{(+)} + (h - \epsilon_0)\Psi^{(+)} = E\Psi^{(+)}. \quad (3.6)$$

The adiabatic approximation neglects the term $(h-\epsilon_0)\Psi^{(+)}$. Equation (3.6) therefore becomes

$$[\epsilon_0 + T + V(\theta,\mathbf{r}) - E]\Psi^{(+)}(\theta,\mathbf{r}) = 0. \quad (3.7)$$

The approximate Hamiltonian employed in (3.7) depends on θ only parametrically. This fact, together with the boundary condition (3.3) leads us to factor $\Psi^{(+)}(\theta,\mathbf{r})$ into two parts:

$$\Psi^{(+)}(\theta,\mathbf{r}) = \Psi_0(\theta)\chi^{(+)}(\theta\mathbf{r}). \quad (3.8)$$

The function $\chi^{(+)}(\theta,\mathbf{r})$ obeys the boundary conditions

$$\chi^{(+)}(\theta,\mathbf{r}) \sim \exp i\mathbf{k}\cdot\mathbf{r} + \text{outgoing waves}. \quad (3.9)$$

Furthermore, substitution of (3.8) into (3.7) yields

$$[T + V(\theta,\mathbf{r}) - (E-\epsilon_0)]\chi^{(+)}(\theta,\mathbf{r}) = 0. \quad (3.10)$$

Equations (3.8), (3.9), and (3.10) constitute the adiabatic approximation.

The validity[19] of the approximation depends on the size of the term that has been neglected in Eq. (3.7), $(h-\epsilon_0)\Psi^{(+)}$. The function $\Psi^{(+)}$ can be expanded into a complete set of rotator states

$$\Psi^{(+)}(\theta,\mathbf{r}) = \sum_i \Psi_i(\theta)\phi_i^{(+)}(\mathbf{r}), \quad (3.11)$$

where the sum extends over all possible rotational excitations coupled in by the interaction $V(\theta,\mathbf{r})$. In terms of this channel representation of $\Psi^{(+)}$, the neglected term becomes

$$(h-\epsilon_0)\Psi^{(+)} = \sum_i (\epsilon_i - \epsilon_0)\Psi_i\phi_i^{(+)}. \quad (3.12)$$

If the channels that are coupled strongly to the entrance channel are of such a nature that $(\epsilon_i - \epsilon_0)$ is much smaller than E, little error is made by neglecting $(h-\epsilon_0)\Psi^{(+)}$ in Eq. (3.7). These criteria are met easily in the case of the scattering of medium-energy projectiles (10–30 MeV) by deformed nuclei. The interaction that couples rotational excitations to the entrance channel is primarily of a quadrupole nature. Thus, only the lowest two or three states of rotational excitation are coupled directly. These states are typically within 200 keV of each other for nuclei in the region $150 < A < 190$, and within 100 keV of each other for nuclei in the region $A > 222$. The excitations of the directly coupled levels are considerably larger for nuclei in the region $A \approx 25$. The excitation energy of the second excited level of the ground-state rotational band of Al^{25} is about 3.4 MeV.

Equation (3.10) has a direct physical interpretation. The projectile is regarded as being scattered by a de-

[19] David M. Chase, Phys. Rev. **104**, 838 (1956).

formed well that has a fixed spatial orientation. The scattering eigenfunction $\chi^{(+)}$ of Eq. (3.10) is a function of the orientation of the well. The full wave function $\Psi^{(+)}$, given by Eq. (3.8), weights $\chi^{(+)}$ with the amplitude of the rotator wave function Ψ_0. Even though the rotator is regarded as fixed for the purposes of calculating $\chi^{(+)}$, the full wave function $\Psi^{(+)}$ has amplitudes in inelastic channels. These are expressed in Eq. (3.11). In other words, the projectile is treated as though it scatters elastically from the rotator, but because the wave function $\chi^{(+)}$ depends on the nuclear orientation, information about the inelastic scattering has been gained.

3.2. Formal Solution to the Adiabatic-Scattering Problem

A partial-wave solution for the wave function $\chi^{(+)}$ will be developed in this section.

It is to our advantage to work with solutions of Eq. (3.10) in the intrinsic coordinate frame; i.e., the coordinate frame that is attached to the rotator and whose quantization axis is along the nuclear symmetry axis.[20] The convention to be adopted is that coordinates that are evaluated relative to the intrinsic frame will be affixed with a prime. The generalized or deformed optical potential then takes the form

$$V(\theta,\mathbf{r})=V(\mathbf{r}'). \tag{3.13}$$

In this form the dependence of $V(\mathbf{r}')$ on the Euler angle θ is implicit. Since the z' axis is along the nuclear symmetry axis, the optical potential $V(\mathbf{r}')$ is also axially symmetric about this axis. Therefore, the projection of the angular momentum of the projectile along the z' axis is a good quantum number.

It is helpful to consider the partial-wave solutions $\chi_{lm}{}^{(+)}$ of Eq. (3.10) that are generated from an incoming wave in one single orbital channel. The orbital angular momentum in this channel is l and its projection onto the z' axis is m. Equation (3.10) becomes

$$[-(\hbar^2/2m)\nabla^2+V(\mathbf{r}')-(E-\epsilon_0)]\chi_{lm}{}^{(+)}(\mathbf{r}')=0. \tag{3.14}$$

However, although m is a good quantum number, l is not. The function $\chi_{lm}{}^{(+)}(\mathbf{r}')$ can be expanded in terms of the spherical harmonics.

$$\chi_{lm}{}^{(+)}(\mathbf{r}')=r^{-1}\sum_{l'} g_{ll'}{}^{m}(r)i^{l'}Y_{l'}{}^{m}(\hat{r}'). \tag{3.15}$$

The boundary conditions obeyed by the $g_{ll'}{}^{m}$ are that

$$g_{ll'}{}^{m}(0)=0$$

at the origin, and that

$$g_{ll'}{}^{m}(r)=(i/2)[\delta_{ll'}H_{l'}{}^{*}(kr)-\xi_{ll'}H_{l'}(kr)] \tag{3.16}$$

when r is outside the range of the nuclear forces. The functions $H_l{}^{*}$ and H_l are, respectively, the incoming and outgoing spherical Coulomb wave functions.[21] The coefficients $\xi_{ll'}$ are generalized reflection coefficients. The wave number k is given by $k=[2m(E-\epsilon_0)/\hbar^2]^{1/2}$. The Coulomb waves have the asymptotic property that

$$H_l\sim\exp i\theta_l$$

and

$$H_l{}^{*}\sim\exp(-i\theta_l),$$

where

$$\theta_l=kr-n\ln(2kr)-l\pi/2+\sigma_l,$$

$$\sigma_l=\arg\Gamma(l+1+in),$$

and

$$n=Zme^2/\hbar^2k.$$

Substitution of Eq. (3.15) into (3.14) yields the coupled system of equations

$$\{-(\hbar^2/2m)[d^2/dr^2-l'(l'+1)/r^2]-(E-\epsilon_0)\}g_{ll'}{}^{m}(r)$$
$$=-\sum_{l''} i^{l''-l'}\langle Y_{l'}{}^{m}|\,V\,|Y_{l''}{}^{m}\rangle g_{ll''}{}^{m}(r). \tag{3.17}$$

Equation (3.17) and the boundary conditions (3.16) uniquely determine the radial waves $g_{ll'}{}^{m}(r)$.

The physical scattering wave function $\chi^{(+)}(\theta,\mathbf{r})$ is a linear combination of the $\chi_{lm}{}^{(+)}(\mathbf{r})$. The expression for $\chi^{(+)}(\theta,\mathbf{r})$ is

$$\chi^{(+)}(\theta,\mathbf{r})=(4\pi/kr)\sum_{lm}(\exp i\sigma_l)Y_l{}^{m*}(\hat{k}')\chi_{lm}{}^{(+)}(\mathbf{r}')$$
$$=(4\pi/kr)\sum_{ll'm}(\exp i\sigma_l)g_{ll'}{}^{m}(r)$$
$$\times Y_l{}^{m*}(\hat{k}')i^{l'}Y_{l'}{}^{m}(\hat{r}'). \tag{3.18}$$

The phase and normalization of (3.18) are chosen so that asymptotically

$$\chi^{(+)}(\theta,\mathbf{r})=\exp i\mathbf{k}\cdot\mathbf{r}+\text{outgoing waves}.$$

The time-reversed wave function is given as usual by the Wigner relation.

$$\chi^{(-)*}(\mathbf{k})=\chi^{(+)}(-\mathbf{k}). \tag{3.19}$$

The formal solution to the adiabatic scattering problem presented here is the full coupled-orbital treatment which is the analog of the coupled-channel treatment of the nonadiabatic theory.

3.3. First-Order Perturbation Solution of the Scattered Waves

Ideally, the full adiabatic wave functions of Eq. (3.8) should be used for $\Psi_i{}^{(+)}$ and $\Psi_f{}^{(-)}$ in Eq. (2.4). However, such a procedure would involve many computational difficulties. Instead, it was decided to treat the departure from sphericity by first-order perturbation theory. Although such a treatment may describe the effects of the inelastic processes inaccurately, it should provide some orientation as to the size of the effects and as to their consequences for the interpretation of stripping-reaction data.

As remarked above, the optical potential well will be taken to have a deformed shape that corresponds to the deformation of the target nucleus. In the phenomenologi-

[20] R. C. Barrett, Nucl. Phys. **51**, 27 (1964).
[21] M. H. Hull and G. Breit, *Handbuch der Physik*, edited by S. Flügge (Springer-Verlag, Berlin, 1959), Vol. 41, Pt. 1, p. 408.

cal theory of Bohr,[22] the deformation of the nuclear surface is described by an angle-dependent nuclear radius. If the deformation has cylindrical symmetry, the nuclear radius is

$$R=R_0[1+\beta Y_l^0(\hat{r}')]. \tag{3.20}$$

It is customary to make a Taylor expansion of the optical potential about the radius R_0, so that

$$V(\mathbf{r}')=V_0(\mathbf{r})+\beta Y_l^0(\hat{r}')R_0(d/dR)V_0(r)+\cdots. \tag{3.21}$$

Here $V_0(r)$ is the optical potential for a spherical nucleus of radius R_0. The potential $V(\mathbf{r}')$ is a generalized optical potential for a deformed nucleus.

The Taylor expansion of the generalized optical potential, (3.21), can be employed in Eq. (3.17). The coupled differential equations for $g_{ll'}{}^m(r)$ then become

$$\{-(\hbar^2/2m)[d^2/dr^2-l'(l'+1)]+V_0(r)-(E-\epsilon_0)\}g_{ll'}{}^m(r) =-\sum_{l''} i^{l''-l'}\langle Y_{l'}{}^m(\hat{r}')|\beta Y_l^0(\hat{r}')R_0(d/dR) \times V_0(r)+\cdots|Y_{l''}{}^m(\hat{r}')\rangle g_{ll''}{}^m(r). \tag{3.22}$$

The partial waves $g_{ll'}{}^m(r)$ also can be expanded in powers of the deformation parameter:

$$g_{ll'}{}^m(r)=\delta_{ll'}f_l(r)+\beta u_{ll'}{}^m(r)+\cdots. \tag{3.23}$$

Here the function $f_l(r)$ describes elastic scattering on a spherical nucleus of radius R_0, and the function $\beta u_{ll'}{}^m(r)$ is the first-order correction to $f_l(r)$ due to the deformation. Substituting Eq. (3.23) for $g_{ll'}{}^m(r)$ in Eq. (3.22) and equating like orders of β yields

$$\{-(\hbar^2/2m)[d^2/dr^2-l(l+1)/r^2] +V_0(r)-(E-\epsilon_0)\}f_l(r)=0, \tag{3.24}$$

and yields

$$\{-(\hbar^2/2m)[d^2/dr^2-l(l+1)/r^2] +V_0(r)-(E-\epsilon_0)\}u_{ll'}{}^m(r) =-i^{l-l'}(5/4\pi)^{1/2}(l/l')\langle lm20|l'm\rangle\langle l020|l'0\rangle \times R_0[(d/dR)V_0(r)]f_l(r). \tag{3.25}$$

At the origin f_l and $u_{ll'}{}^m$ obey the boundary conditions

$$f_l(0)=u_{ll'}{}^m(0)=0. \tag{3.26}$$

Beyond the range of the nuclear interaction, they obey

$$f_l(r)=\tfrac{1}{2}i[H_l^*(kr)-\eta_l H_l(kr)], \tag{3.27}$$

and

$$U_{ll'}{}^m(r)\propto H_l(kr). \tag{3.28}$$

The vector-coupling coefficients in Eq. (3.25) impose the conditions

$$l'=l, l\pm 2. \tag{3.29}$$

Parity is a good quantum number for all orders of the expansion in β, because the nuclear interaction is even under inversion of the coordinate axes.

[22] Aage Bohr, Kgl. Danske Videnskab. Selskab, Mat. Fys. Medd. **26**, No. 14 (1952).

It is highly desirable to separate $u_{ll'}{}^m(r)$ into a geometric factor and a radial function that is independent of m. This is possible because the terms in Eq. (3.25) that are homogeneous in $u_{ll'}{}^m(r)$ do not themselves depend upon m. Then

$$u_{ll'}{}^m(r)\equiv i^{l-l'}(5/4\pi)^{1/2}\hat{l}/\hat{l}'\langle lm20|l'm\rangle \times\langle l020|l'0\rangle R_0 v_{ll'}(r). \tag{3.30}$$

The function $v_{ll'}(r)$ satisfies a simplified differential equation:

$$\{-\hbar^2/2m[d^2/dr^2-l'(l'+1)/r^2]+V_0(r)-(E-\epsilon_0)\} \times v_{ll'}(r)=-[(d/dR)V_0(r)]f_l(r). \tag{3.31}$$

The boundary conditions on $v_{ll'}(r)$ are the same as those on $u_{ll'}{}^m(r)$. Although the function $v_{ll'}(r)$ does not itself reflect the nonspherical shape of the nuclear interaction, it does contain all aspects of the dependence of $u_{ll'}{}^m(r)$ on the strength of the optical potential and on the variation of the potential with respect to radius parameter.

The physical scattered wave $\chi^{(+)}$ may now be evaluated to first order in β.

$$\chi^{(+)}(\theta,\mathbf{r})=\chi_0{}^{(+)}(\mathbf{r})+\beta\chi_1{}^{(+)}(\theta,\mathbf{r})+\cdots. \tag{3.32}$$

Substitution of Eq. (3.23) for $g_{ll'}{}^m(r)$ in Eq. (3.18) yields

$$\chi_0{}^{(+)}(\mathbf{r})=(4\pi/kr)\sum_{lm}(\exp i\sigma_l) \times f_l(r)Y_l{}^{m*}(\hat{k})i^lY_l{}^m(r), \tag{3.33}$$

and

$$\chi_1{}^{(+)}(\theta,\mathbf{r})=(4\pi/kr)\sum_{ll'm}(\exp i\sigma_l) \times u_{ll'}{}^m(r)Y_l{}^{m*}(\hat{k}')i^{l'}Y_{l'}{}^m(\hat{r}'). \tag{3.34}$$

Equation (3.33) is the familiar partial-wave expansion of a wave function that describes elastic scattering by a spherical nucleus. In Eq. (3.34) the dependence of $\chi_1{}^{(+)}$ on the Euler angles is implicit, insomuch as $\hat{k}'$ and $\hat{r}'$ are functions of θ.

For later use, Eq. (3.34) will be rewritten in order to exhibit explicitly its dependence on the Euler angles. The spherical harmonics in (3.34) are transformed to the space-fixed frame and Eq. (3.30) is substituted for $u_{ll'}{}^m(r)$. After some standard Racah algebra is performed, Eq. (3.34) becomes

$$\chi_1{}^{(+)}(\theta,\mathbf{r})=(4\pi/kr)\sum_{lml'm'\alpha} i^{l-l'}(5/4\pi)^{1/2}(l/l') \times\langle lm2-\alpha|l'm\rangle\langle l020|l'0\rangle\mathfrak{D}_{-\alpha 0}{}^{2*}(\theta)(\exp i\sigma_l) \times R_0 v_{ll'}(r)Y_l{}^{m*}(\hat{k})i^{l'}Y_{l'}{}^{m'}(\hat{r}'). \tag{3.35}$$

The time-reversed scattering functions that correspond to Eqs. (3.33) and (3.35) are given by the Wigner relation, Eq. (3.19).

$$\chi_0{}^{(-)*}(\mathbf{r})=(4\pi/kr)\sum_{lm}(\exp i\sigma_l) \times f_l(r)Y_l{}^m(\hat{k})i^{-l}Y_l{}^{m*}(\hat{r}). \tag{3.36}$$

$$\chi_1{}^{(-)*}(\theta,\mathbf{r})=(4\pi/kr)\sum_{lml'm'\alpha} i^{l'-l}(5/4\pi)^{1/2}(\hat{l}/\hat{l}') \times\langle lm2-\alpha|l'm'\rangle\langle l020|l'0\rangle\mathfrak{D}_{-\alpha 0}{}^2(\theta)(\exp i\sigma_l) \times R_0 v_{ll'}(r)Y_l{}^m(\hat{k})i^{-l'}Y_{l'}{}^{m'*}(\hat{r}). \tag{3.37}$$

4. ANALYSIS OF THE STRIPPING MODEL

In this section, the deuteron stripping amplitude will be formulated to first-order in the deformation parameter[22] β. An approximation will be introduced which will considerably simplify the first-order amplitudes. The effects of nonlocality of the optical potential will be analyzed and it will be seen that these effects add little complication to the stripping amplitude.

4.1. Adiabatic Stripping Amplitude

In this subsection, the transition amplitude for the stripping process will be cast in the language of the adiabatic approximation. The amplitude of Eq. (2.4) is rewritten, in slightly modified form, as

$$T_{dp}=(N+1)^{1/2}(\Psi_f^{(-)}(n,p,\theta,\xi),V_{np}\Psi_i^{(+)}(n,p,\theta,\xi)). \quad (4.1)$$

In this expression the Euler angles are displayed explicitly. The coordinates ξ are now to be thought of as only the intrinsic coordinates of the deformed target nucleus. The asymptotic boundary conditions obeyed by the initial and final wave functions are

$$\begin{aligned}\Psi_i^{(+)}&\sim S_{\mu_d}(\sigma_n,\sigma_p)\phi_{np}(r_{np})\Psi_A(\theta,\xi)\\&\quad\times\exp i\mathbf{k}_d\cdot\mathbf{r}_d+\text{outgoing waves}.\\\Psi_f^{(-)}&\sim S_{\mu_p}(\sigma_p)\Psi_B(n,\theta,\xi)\\&\quad\times\exp i\mathbf{k}_p\cdot\mathbf{r}_p+\text{incoming waves}.\end{aligned} \quad (4.2)$$

In close analogy with Eq. (3.5), the Schrödinger equation for the entrance-channel wave function is

$$\{h_1(\theta,\xi)+(T_{np}+V_{np})+[T_d+V_d(\theta,\mathbf{r}_d)]-E\}\Psi_i^{(+)}(n,p,\theta,\xi)=0. \quad (4.3)$$

The portion h_1 is the Hamiltonian for the isolated target nucleus; i.e.,

$$[h_1(\theta,\xi)-\epsilon_A]\Psi_A(\theta,\xi)=0. \quad (4.4)$$

The term T_{np} is the kinetic-energy operator for the deuteron internal motion, so that

$$(T_{np}+V_{np}-\epsilon_d)\phi_{np}=0. \quad (4.5)$$

The term T_d is the kinetic-energy operator for the deuteron center-of-mass motion. The initial wave function then becomes a product of three factors:

$$\Psi_i^{(+)}=S_{\mu_d}(\sigma_n,\sigma_p)\phi_{np}\Psi_1^{(+)}(\theta,\xi,\mathbf{r}_d). \quad (4.6)$$

The asymptotic boundary conditions for the factor $\Psi_1^{(+)}$ are

$$\Psi_1^{(+)}\sim\Psi_A(\theta,\xi)\exp i\mathbf{k}_d\cdot\mathbf{r}_d+\text{outgoing waves}. \quad (4.7)$$

The Schrödinger equation for $\Psi_1^{(+)}$ is

$$[h_1(\theta,\xi)+T_d+V_d(\theta,\mathbf{r}_d)-(E-\epsilon_d)]\Psi_1^{(+)}(\theta,\xi,\mathbf{r}_d)=0. \quad (4.8)$$

Similarly, the Schrödinger equation for the exit-channel wave function is

$$[h_2(\theta,n,\xi)+T_p+V_p(\theta,\mathbf{r}_p)-E]\Psi_f^{(-)\dagger}(n,p,\theta,\xi)=0. \quad (4.9)$$

The operator h_2 is the Hamiltonian for the isolated product nucleus:

$$[h_2(\theta,n,\xi)-\epsilon_B]\Psi_B(\theta,n,\xi)=0. \quad (4.10)$$

The term T_p is the kinetic-energy operator for the proton. The final wave function is a product of two factors:

$$\Psi_f^{(-)}=S_{\mu_p}(\sigma_p)\Psi_2^{(-)}(\theta,n,\xi,\mathbf{r}_p). \quad (4.11)$$

As in Sec. 3, the adiabatic approximation will be used in the evaluation of $\Psi_1^{(+)}$ and $\Psi_2^{(-)}$:

$$\begin{aligned}\Psi_1^{(+)}&\approx\Psi_A(\theta,\xi)\chi^{(+)}(\theta,\mathbf{r}_d),\\\Psi_2^{(-)}&\approx\Psi_B(\theta,n,\xi)\chi^{(-)}(\theta,\mathbf{r}_p).\end{aligned} \quad (4.12)$$

In Eq. (4.12) the separation of the projectile coordinates from the intrinsic coordinates of the target nuclei is complete. Only rotational inelastic excitations are being accounted for. The Schrödinger equations for the quasi-elastic scattering wave functions are:

$$\begin{aligned}[T_d+V_d(\theta,\mathbf{r}_d)-(E-\epsilon_d-\epsilon_A)]\chi_A^{(+)}(\theta,\mathbf{r}_d)=0,\\[T_p+V_p(\theta,\mathbf{r}_p)-(E-\epsilon_B)]\chi_B^{(-)*}(\theta,\mathbf{r}_p)=0.\end{aligned} \quad (4.13)$$

The solutions of Eqs. (4.13) were discussed in Sec. 3.

The adiabatic transition amplitude is obtained by substituting Eqs. (4.6), (4.11), and (4.12) for $\Psi_i^{(+)}$ and $\Psi_f^{(-)}$ in Eq. (4.1):

$$T_{dp}=(N+1)^{1/2}(S_{\mu_p}(\sigma_p)\Psi_B(\theta,n,\xi)\chi^{(-)}(\theta,\mathbf{r}_p),V_{np}S_{\mu_d}(\sigma_n,\sigma_p)\phi_{np}\Psi_A(\theta,\xi)\chi^{(+)}(\theta,\mathbf{r}_d)). \quad (4.14)$$

Equation (4.14) lends itself to qualitative physical interpretation. In order to avoid unnecessary clutter in the discussion the nucleons will be assumed, for now, to be spinless particles and the bound-state wave functions will be chosen simply to be

$$\Psi_A(\theta,\xi)=\mathfrak{D}_A(\theta)\psi_A(\xi'), \quad (4.15)$$

and

$$\Psi_B(\theta,n,\xi)=\mathfrak{D}_B(\theta)\psi_B(\mathbf{r}_n',\xi'). \quad (4.16)$$

The functions $\mathfrak{D}_A$ and $\mathfrak{D}_B$ are rotational wave functions and represent the probability amplitudes of the orientations of the target and product nuclei, respectively. The wave functions ψ_A and ψ_B are intrinsic wave functions. Their arguments are primed in order to emphasize that these functions represent intrinsic configurations. For these simple wave functions Eq. (4.14) becomes

$$T_{dp}=\int d^3\theta\ \mathfrak{D}_B^*(\theta)T_\theta\mathfrak{D}_A(\theta), \quad (4.17)$$

where

$$T_\theta=(N+1)^{1/2}(\chi^{(-)}(\theta,\mathbf{r}_p),\langle\psi_B(\mathbf{r}_n',\xi')|\psi_A(\xi')\rangle D_{np}\chi^{(+)}(\theta,\mathbf{r}_d)), \quad (4.18)$$

and

$$D_{np}\equiv V_{np}\phi_{np}.$$

Because $\chi^{(-)}$ and $\chi^{(+)}$ can be regarded as describing scattering by a fixed deformed well, T_θ can be thought of as the transition amplitude for stripping on a deformed

nucleus whose orientation in space is fixed. In other words, the model assumes that the deformed nucleus rotates by a negligible degree in the time required for the stripping reaction to take place. The true stripping amplitude T_{dp} is found by weighting T_θ by the probability amplitudes of the orientations of the target and product nuclei.

Returning now to the development of the transition amplitude, Eq. (4.14) is expanded up to first order in β. Substitution of (3.32) for $\chi^{(+)}$ and a similar expression for $\chi^{(-)}$ yields

$$T_{dp}=T_0+\beta T_1+\cdots, \tag{4.19}$$

where

$$T_0=(N+1)^{1/2}(S_{\mu_p}\Psi_B\chi_0^{(-)},D_{np}S_{\mu_d}\Psi_A\chi_0^{(+)}), \tag{4.20}$$

and

$$T_1=(N+1)^{1/2}[(S_{\mu_p}\Psi_B\chi_1^{(-)},D_{np}S_{\mu_d}\Psi_A\chi_0^{(+)}) +(S_{\mu_p}\Psi_B\chi_0^{(-)},D_{np}S_{\mu_d}\Psi_A\chi_1^{(+)})]. \tag{4.21}$$

The amplitude T_0 is the familiar distorted-wave Born approximation amplitude for the stripping reaction. The amplitude T_1 is the first-order term in a perturbation expansion of T_{dp} in the deformation parameter. It is the first-order approximation of the contributions of the inelastic channels to the stripping amplitude.

4.2. Zero-Order Amplitude

The results of the integrations over the θ, ξ, and spin coordinates in Eq. (4.20) will be presented. Equation (4.20) is just the zero-order term in the stripping amplitude for a deformed target nucleus and has previously been studied by Satchler.[12] The amplitude T_0 is zero order in β, insofar as the scattering of the incident deuteron and the exit proton are treated to zero order in β. However, a Nilsson wave function is used for the captured-neutron orbital.

The strong-coupling wave function for a deformed nucleus is[12,23]

$$\Psi=(\hat{I}/4\pi)\phi_{\text{vib}}[\mathfrak{D}_{MK}^{I}(\theta)\psi_\Omega(\xi') +(-1)^{I-\frac{1}{2}A}\mathfrak{D}_{M-K}^{I}(\theta)\psi_{-\Omega}(\xi')], \tag{4.22}$$

where A is the atomic number of the nucleus, $\hat{I}\equiv(2I+1)^{1/2}$, and

$$\psi_\Omega=\phi_p(p_1\cdots p_Z)\phi_n(n_1\cdots n_N). \tag{4.23}$$

The wave functions ϕ_p and ϕ_n are antisymmetrized products of single-particle orbitals. More explicitly, the neutron wave function is

$$\phi_n=\mathfrak{A}[U(n_1)\cdots U(n_N)], \tag{4.24}$$

where $\mathfrak{A}$ is the antisymmetrization operator. The single-particle wave functions U_Ω are not completely specified by Ω; however any other quantum numbers that are needed to specify U_Ω may conveniently be left implied. The proton wave function has a similar structure.

[23] Aage Bohr and Ben R. Mottelson, Kgl. Danske Videnskab. Selskab, Mat. Fys. Medd. **27**, No. 16 (1953).

The angular momentum of an orbital of a deformed well is not, generally, a good quantum number. In terms of functions that do have definite angular momentum,

$$U_\Omega(n_i)=\sum_{lj}C_{lj}(\Omega)\{\psi_l(\mathbf{r}_i),S_{1/2}(\sigma_i)\}_j^\Omega, \tag{4.25}$$

where ψ_l is an orbital function and $S_{1/2}$ is a nucleon spin function. The wave function $\{\psi_l,S_{1/2}\}_j^\Omega$ is constructed by vector coupling the orbital and spin angular momenta of the ith neutron:

$$\{\psi_l,S_{1/2}\}_j^\Omega=\sum_m\langle lm\tfrac{1}{2}\Omega-m\,|\,j\Omega\rangle\psi_{lm}S_{\frac{1}{2}\Omega-m}.$$

Therefore in the uncoupled representation

$$U_\Omega=\sum_{lm}a_{lm}(\Omega)\psi_{lm}S_{\frac{1}{2}\Omega-m}, \tag{4.26}$$

where

$$a_{lm}(\Omega)=\sum_j\langle lm\tfrac{1}{2}\Omega-m\,|\,j\Omega\rangle C_{lj}(\Omega). \tag{4.27}$$

By using a specific model for the deformed single-particle potential, Nilsson calculated the coefficients $a_{lm}(\Omega)$ for the eight major shells of nuclei, as a function of the nuclear deformation.[11]

The intrinsic wave function $\psi_{-\Omega}(\xi')$ of Eq. (4.22) is equivalent to $\psi_\Omega(\xi')$ except that the sign of the projection quantum number of each orbital is reversed. The phase connection used for each of the single-particle orbitals in $\psi_{-\Omega}$ is

$$C_{lj}(-\Omega)=(-1)^{j-\frac{1}{2}}C_{lj}(\Omega). \tag{4.28}$$

For nonzero overlap, the intrinsic wave functions of the target and product nuclei must not differ by more than one neutron orbital U_Ω. Furthermore, $\Omega=\Omega_2\mp\Omega_1$; where Ω_1 and Ω_2 are the projections onto the symmetry axis of the intrinsic angular momenta of the target and product nuclei, respectively. Let us assume that the radius and deformation of the product nucleus are only slightly different from the corresponding radius and deformation of the target nucleus. Then $\phi_{\text{vib}}{}^A$, which describes the zero-point oscillations of the target nucleus, will have close to unit overlap with $\phi_{\text{vib}}{}^B$, which describes the zero-point oscillations of the product nucleus. In what follows, $\langle\phi_{\text{vib}}{}^B\,|\,\phi_{\text{vib}}{}^A\rangle$ will therefore be taken as unity.

The integration of Eq. (4.20) over the target coordinates and the neutron spin coordinate now is straightforward, and gives[12]

$$T_0=g(\hat{I}_1/\hat{I}_2)\sum_{JMJ\mu_n}\langle\tfrac{1}{2}\mu_n\tfrac{1}{2}\mu_p\,|\,1\mu_d\rangle \times\langle I_1M_1JM_J\,|\,I_2M_2\rangle\langle I_1\pm K_1J\Omega\,|\,I_2K_2\rangle \times\sum_{LM}\langle LM\tfrac{1}{2}\mu_n\,|\,JM_J\rangle C_{LJ}(\Omega)t_0{}^{LM}. \tag{4.29}$$

The factor g has the value $g=\sqrt{2}$ if either the target or the product nucleus is even-even, with all of its intrinsic orbitals paired; otherwise, $g=1$. The "single-particle transition amplitude" of Eq. (4.29) is given by

$$t_0{}^{LM}=(\chi_0^{(-)}(\mathbf{r}_p), i^{-L}Y_L{}^{M*}(\hat{r}_n)F_L(r_n)D_{np}\chi_0^{(+)}(\mathbf{r}_d)). \tag{4.30}$$

The entire dependence of T_0 upon scattering angle is carried by these single-particle amplitudes. The remaining factors in (4.29) are weighting factors that measure how well the bound wave functions overlap. After D_{np} is replaced by its zero-range approximation and the scattering wave functions are replaced by their partial-wave expansions, (3.33) and (3.36), Eq. (4.30) becomes

$$t_0^{LM}=A[(4\pi)^{3/2}/k_pk_d]\sum_{l_1m_1l_2m_2} i^{l_1-L-l_2}(\hat{l}_2\hat{L}/\hat{l}_1) \times\langle l_2m_2LM\,|\,l_1m_1\rangle\langle l_20L0\,|\,l_10\rangle Y_{l_2}^{m_2}(\hat{k}_p) \times Y_{l_1}^{m_1*}(\hat{k}_d)I_0(l_2,L,l_1), \quad (4.31)$$

where

$$D_{np}\approx A\,\delta(\mathbf{r}_n-\mathbf{r}_p), \qquad A\equiv-(4\pi)^{1/2}(\hbar^2/M)N, \quad (4.32)$$

and

$$I_0(l_2,L,l_1)=[\exp i(\sigma_{l_1}+\sigma_{l_2})] \times\int_0^\infty dr\, f_{l_2}(r)F_L(r)f_{l_1}(r). \quad (4.33)$$

The factor A is the strength of D_{np}. The mass M is the mass of a nucleon and N is the asymptotic normalization of the deuteron internal wave function.[24]

4.3. First-Order Amplitude

In this subsection, the integrations over the θ, ξ, and spin coordinates in Eq. (4.21) will be presented. The amplitude T_1 is first order in β, insofar as the scattering of the incident and exit projectiles are treated to first order in β. In other words, T_1 is a first-order perturbative correction to T_0, due to the coupling of the projectile motion to the rotational motion of the deformed nucleus, in both the entrance and exit channels.

The continuum wave functions of (4.21) are replaced by Eqs. (3.33), (3.35), (3.36), and (3.37). Equation (4.21) then becomes

$$T_1=g(\hat{I}_1/\hat{I}_2)\sum_{JM_J\mu_n}\langle\tfrac{1}{2}\mu_n\tfrac{1}{2}\mu_p\,|\,1\mu_d\rangle \times\langle I_1M_1JM_J\,|\,I_2M_2\rangle\langle I_1\pm K_1J\Omega\,|\,I_2K_2\rangle \times\sum_{LM}\langle LM\tfrac{1}{2}\mu_n\,|\,JM_J\rangle t_1^{LM}(J), \quad (4.34)$$

where

$$t_1^{LM}(J)=\sum_{lm}(5/4\pi)^{1/2}\langle Lm\tfrac{1}{2}\Omega-m\,|\,J\Omega\rangle\langle Lm20\,|\,lm\rangle a_{lm}(\Omega) \times\{A[(4\pi)^{3/2}/k_pk_d]\sum_{l_1m_1l_2m_2}(2L+1)\hat{l}_2\langle l_2m_2LM\,|\,l_1m_1\rangle Y_{l_2}^{m_2}(\hat{k}_p)Y_{l_1}^{m_1*}(\hat{k}_d) \times[\textstyle\sum_{l_1'} i^{l_1-l-l_2}\langle l_1020\,|\,l_1'0\rangle\langle l_20l0\,|\,l_1'0\rangle W(l_1l_1'Ll;\,2l_2)R_dI_d(l_2,l,l_1l_1') \times(-1)^{L+l}\textstyle\sum_{l_2'} i^{l_2-l-l_1}\langle l_2020\,|\,l_2'0\rangle\langle l_10l0\,|\,l_2'0\rangle W(l_2l_2'Ll;\,2l_1)R_pI_p(l_2l_2',l,l_1)]\}. \quad (4.35)$$

The radial overlaps in Eq. (4.35) are given by

$$I_d=[\exp i(\sigma_{l_1}+\sigma_{l_2})]\int_0^\infty dr\, f_{l_2}(r)F_l(r)v_{l_1l_1'}(r), \quad (4.36)$$

and

$$I_p=[\exp i(\sigma_{l_1}+\sigma_{l_2})]\int_0^\infty dr\, v_{l_2l_2'}(r)F_l(r)f_{l_1}(r). \quad (4.37)$$

Equation (4.35) shows that the orbital angular momentum transfer L is not necessarily equal to the orbital angular momentum l of the captured nucleon. Instead, the selection rule for the orbital angular momentum transfer is

$$|l-2|\leq L\leq l+2.$$

In addition, the orbital angular momentum transfer L does not carry the parity of the first-order transition as it did for the zero-order transition. Instead, the parity is carried by l.

4.4. Approximate First-Order Amplitude

The first-order amplitude (4.35) is an unwieldy expression. In this section, a simplified approximate form for Eq. (4.35) will be developed.

The term in brackets in Eq. (4.35) involves two sums over very similar expressions. In each sum, the summation index appears both in the vector-coupling coefficients and in the radial integrals. The vector-coupling coefficients are very sensitive functions of the summation indices. In fact, the product of these coefficients is nonzero only for[25] $l'=l, l\pm2$. It will be assumed that the variation of the radial integrals over the allowed range of l' is sufficiently small that the integrals may be assumed independent of l'.

[24] N. Austern, in *Fast Neutron Physics, II*, edited by J. B. Marion and J. L. Fowler (Interscience Publishers, Inc., New York, 1962).

[25] Due to the symmetry of the two summations, the discussion is the same for both; hence the subscripts 1 and 2 are dropped from l and l'.

It is evident from (4.36) and (4.37) that this approximation essentially replaces $v_{ll'}$ by v_{ll}. In order to have a better understanding of the approximation let us consider the integral expression for $v_{ll'}$.

$$v_{ll'}(r)=-(1/k)\int_0^\infty dr\, f_{l'}(r_<)h_{l'}(r_>)[dV_0(r)/dR]f_l(r). \tag{4.38}$$

The function $h_{l'}$ is the homogeneous solution to (3.31) that behaves asymptotically as

$$h_{l'}(r)\sim H_{l'}(kr). \tag{4.39}$$

The interaction $dV_0(r)/dR$ is localized to the nuclear surface, hence the dependence of $v_{ll'}$ on l' is contained largely in the Green's function in the region of the surface. In this region the phase of the Green's function for the lowest partial waves depends strongly on l'. However, as the centrifugal barrier pushes closer to the surface, the Green's function adopts a weaker dependence on l'. Consequently, it is not a bad approximation to replace l' by l, provided that l' is in the neighborhood of l and provided that the centrifugal barrier is near the surface.[26] In spite of the fact that the approximation is probably poor for the low partial waves, it will be adopted, on the grounds that it should at least be accurate enough to serve as a first attempt toward understanding the effects of the nuclear deformation on the stripping reaction.

Under the approximation that $v_{ll'}=v_{ll}$, Eq. (4.35) can be simplified with the use of the Racah formula:

$$\sum_f \hat{e}\hat{f}\langle a\alpha f\gamma-\alpha|c\gamma\rangle\langle b\beta d\gamma-\alpha-\beta|f\gamma-\alpha\rangle W(abcd;ef)=\langle a\alpha b\beta|e\alpha+\beta\rangle\langle e\alpha+\beta d\gamma-\alpha-\beta|c\gamma\rangle. \tag{4.40}$$

It then becomes

$$\begin{aligned} t_1^{LM}(J)=(5/4\pi)^{1/2}\sum_{LM} i^{L-l}a_{lm}(\Omega)\langle Lm\tfrac{1}{2}\Omega-m|J\Omega\rangle\langle Lm20|lm\rangle\langle l020|L0\rangle \\ \times\{A[(4\pi)^{3/2}/k_pk_d]\sum_{l_1m_1l_2m_2} i^{l_1-L-l_2}(\hat{L}\hat{l}_2/\hat{l}_1)\langle l_2m_2LM|l_1m_1\rangle\langle l_20L0|l_10\rangle \\ \times Y_{l_2}^{m_2}(\hat{k}_p)Y_{l_1}^{m_1*}(\hat{k}_d)[R_pI_p(l_2l_2,l,l_1)+R_d(l_2,l,l_1l_1)]\}. \end{aligned} \tag{4.41}$$

The orbital angular momentum transfer L is now restricted to carry the parity transfer. The loss of the non-normal parity amplitudes is inconsequential because in any case these amplitudes would not interfere coherently with the direct amplitudes. The factor in curly brackets in (4.41) now has a structure very much the same as the single-particle stripping amplitude t_0^{LM} of Eq. (4.31). The difference between the two quantities rests in the radial integrals.

It will be demonstrated now that the factor in the curly brackets in (4.41) is equivalent to a derivative operation on a generalized single-particle transition amplitude. Let us consider the differential equation that the partial wave f_l obeys:

$$\{-(\hbar^2/2m)[d^2/dr^2-l(l+1)/r^2]+V_0(r)-(E-\epsilon_0)\}f_l(r)=0. \tag{3.24}$$

Let us suppose that the radius of the optical potential is given a scalar increment h such that the potential remains spherically symmetric. If we expand in powers of h, and solve for f_l as a function of h, then

$$V(R_0+h,r)=V_0(r)+hdV_0/dR+\cdots, \tag{4.42}$$

and

$$\left\{-\frac{\hbar^2}{2m}\left[\frac{d^2}{dr^2}-\frac{l(l+1)}{r^2}\right]+\left[V_0(r)+h\frac{dV_0(r)}{dR}+\cdots\right]-(E-\epsilon_0)\right\}f_l(R_0+h,r)=0. \tag{4.43}$$

In (4.43) the dependence of f_l on R has been given explicit acknowledgment. As was done for V, f_l is expanded in powers of h:

$$f_l(R_0+h,r)=f_l(r)+hdf_l(r)/dR+\cdots, \tag{4.44}$$

where it is to be understood that $f_l(r)$ on the right-hand side of (4.44) is equivalent to $f_l(R_0,r)$. Substituting (4.44) into (4.43) and equating first-order terms in h yields

$$\{-(\hbar^2/2m)[d^2/dr^2+l(l+1)/r^2]+V_0(r)-(E-\epsilon_0)\}df_l(r)/dR=-[dV_0(r)/dR]f_l(r). \tag{4.45}$$

The differential equation that $df_l(r)/dR$ obeys now is seen to be the same one that $v_{ll}(r)$ obeys. Moreover, both $df_l(r)/dR$ and $v_{ll}(r)$ obey the same boundary conditions. Therefore,

$$v_{ll}(r)=df_l(r)/dR, \tag{4.46}$$

and the radial integrals in (4.41) are given by

$$R_pI_p(l_2l_2,l,l_1)+R_dI_d(l_2,l,l_1l_1)=(R_pd/dR_p+R_dd/dR_d)I_0(l_2,l,l_1). \tag{4.47}$$

[26] N. Austern and J. S. Blair, Ann. Phys. (N.Y.) 33, 15 (1965).

Using (4.47), the factor in curly brackets, { }, in (4.41) becomes

$$\{\ \}=(R_p d/dR_p+R_d d/dR_d)t_l^{LM}, \tag{4.48}$$

where the generalized single-particle stripping amplitude is given by

$$t_l^{LM}=A[(4\pi)^{3/2}/k_p k_d]\sum_{l_1 m_1 l_2 m_2} i^{l_1-L-l_2}(\hat{L}\hat{l}_2/\hat{l}_1)\langle l_2 m_2 LM\,|\,l_1 m_1\rangle\langle l_2 0 L0\,|\,l_1 0\rangle Y_{l_2}^{m_2}(\hat{k}_p)Y_{l_1}^{m_1*}(\hat{k}_d)I_0(l_2,l,l_1). \tag{4.49}$$

The amplitude t_l^{LM} is generalized from t_0^{LM} in the sense that it reduces to t_0^{LM} in the case that $l=L$.

Using (4.48), Eq. (4.41) becomes

$$t_1^{LM}(J)=(5/4\pi)^{1/2}\sum_{lm} i^{l-L}a_{lm}(\Omega)\langle Lm\tfrac{1}{2}\Omega-m\,|\,J\Omega\rangle\langle Lm20\,|\,lm\rangle\langle l020\,|\,L0\rangle(R_p d/dR_p+R_d d/dR_d)t_l^{LM}. \tag{4.50}$$

Substitution of (4.50) for $t_1^{LM}(J)$ in (4.34) and subsequent substitution of (4.34) and (4.29) into (4.19) yields

$$\begin{aligned}T_{dp}\approx g(\hat{I}_1/\hat{I}_2)&\sum_{JM_J\mu_n}(\tfrac{1}{2}\mu_n\tfrac{1}{2}\mu_p\,|\,1\mu_d)\langle I_1M_1JM_J\,|\,I_2M_2\rangle\langle I_1\pm K_1J\Omega\,|\,I_2K_2\rangle\\ &\times\sum_{LM}\langle LM\tfrac{1}{2}\mu_n\,|\,JM_J\rangle\sum_{lm}\langle Lm\tfrac{1}{2}\Omega-m\,|\,J\Omega\rangle a_{lm}(\Omega)\\ &\times[\delta_{lL}t_L^{LM}+i^{L-l}(5/4\pi)^{1/2}\beta\langle Lm20\,|\,lm\rangle\langle l020\,|\,L0\rangle(R_p d/dR_p+R_d d/dR_d)t_l^{LM}].\end{aligned} \tag{4.51}$$

It is emphasized here that (4.51) is an approximation to a first-order theory.

This expression for T_{dp} is closely analogous to Eq. (4b) of the paper of Sawicki and Satchler.[13] However, instead of using a distorted-wave treatment of the initial- and final-state wave functions, they employ the Butler prescription. The fact that (4.51) has a phase factor i^{L-l} that multiplies the first-order contributions, whereas (4b) of Sawicki and Satchler does not, is simply a reflection of the fact that those authors employ Nilsson's[11] phase convention for $a_{lm}(\Omega)$. The Nilsson coefficients are expansion coefficients in terms of the spherical functions $F_l(r)Y_l^m(\hat{r})S_{\frac{1}{2}\Omega-m}(\sigma_n)$; whereas the coefficients $a_{lm}(\Omega)$ employed in (4.51) are expansion coefficients in terms of $F_l(r)i^lY_l^m(\hat{r})S_{\frac{1}{2}\Omega-m}(\sigma)$. Therefore the $a_{lm}(\Omega)$ of (4.51) are obtained if the Nilsson coefficients are multiplied by i^{-l}. Because of the essential similarity between (4.51) and the results of Sawicki and Satchler, the discussion presented in their paper applies equally to (4.51).

It may be significant that the approximation introduced in this section yields a result very much like the plane-wave result. Under the conditions of strong absorption, the low partial waves are suppressed and the main contributions to (4.35) come from those partial waves whose orbital angular momenta are near the classical cutoff value.[27] Hence, under the conditions of strong absorption, (4.41) is expected to be a good approximation to (4.35).[26] Because of the suppression of the low partial waves, contributions from the nuclear interior are very small.[27] In this respect, distorted-wave theory with strong absorption is similar to the plane-wave theory.

4.5. Nonlocal Optical Potentials

The nuclear optical potential probably is nonlocal; i.e., the Schrödinger equation for elastic scattering probably should be

$$-(\hbar^2/2m)\nabla^2\chi(\mathbf{r})+I(\mathbf{r})=E\chi(\mathbf{r}), \tag{4.52}$$

where

$$I(\mathbf{r})=\int d^3r'\ V_{NL}(\mathbf{r},\mathbf{r}')\chi(\mathbf{r}'). \tag{4.53}$$

A prominent effect of the nonlocality is a damping of the scattering wave function inside the nucleus. In this section, the effects of the deformation on the stripping reaction will be analyzed insofar as the deformation modifies the damping of the initial and final wave functions.

Perey and Buck[28] investigated a particular factorable form for the nonlocality:

$$V_{NL}=V(|\tfrac{1}{2}[\mathbf{r}+\mathbf{r}']|)H(|\mathbf{r}'-\mathbf{r}|). \tag{4.54}$$

The potential V describes the shape and strength of the interaction and H carries the range γ of the nonlocality. The factor H is normalized so that

$$\int d^3s\ H(s)=1, \tag{4.55}$$

where

$$s=|\mathbf{r}'-\mathbf{r}|.$$

In the local approximation, $H(s)=\delta^3(s)$; i.e., $\gamma=0$. As γ varies, V must be adjusted in order that the asymptotic behavior of χ should remain constant. Therefore, V is a function of the range of the nonlocality. In addition, it has been exhibited both numerically[29] and analytically[30,31] that the scattering wave function is damped in the nuclear interior as the nonlocality is "turned on." In these treatments, H was chosen to have a Gaussian dependence on s. The analysis introduces a function

[27] N. Austern, in *Selected Topics in Nuclear Theory*, edited by F. Janouch (International Atomic Energy Agency, Vienna, 1963).

[28] F. G. Perey and B. Buck, Nucl. Phys. **32**, 353 (1962).

[29] F. G. Perey, in *Direct Interactions and Nuclear Reaction Mechanism*, edited by E. Clementel and C. Villi (Gordon and Breach, Science Publishers. Inc., New York, 1963), p. 125.

[30] N. Austern, Phys. Rev. **137**, B752 (1965).

[31] F. G. Perey and D. S. Saxon, Phys. Letters **10**, 107 (1964).

$F(\gamma,\mathbf{r})$ which describes the modification of the local wave function as the nonlocality is turned on.

$$\chi(\gamma,\mathbf{r})=F(\gamma,\mathbf{r})\chi(\mathbf{r}). \tag{4.56}$$

The wave function $\chi(\mathbf{r})$ on the right-hand side of (4.56) is understood to be the local wave function; i.e. $\chi(\mathbf{r})=\chi(\gamma=0,\mathbf{r})$. The function $F(\gamma,\mathbf{r})$ goes to unity outside the range of the nuclear interactions. An explicit, general expression for F can be obtained in WKB approximation:

$$F(\gamma,\mathbf{r})=[1-\tfrac{1}{4}\gamma^2(2m/\hbar^2)V(\mathbf{r})]^{-1/2}, \tag{4.57}$$

where $V(\mathbf{r})$ is the local approximation to the nonlocal potential.

The local scattering functions in (4.14) will now be replaced by the nonlocal wave functions. Using Eq. (4.56) and the WKB approximation of $F(\gamma,\mathbf{r})$, the transition amplitude becomes

$$T_{dp}=(N+1)^{1/2}\langle S_{\mu_p}(\sigma_p)\Psi_B(\theta,n,\xi)F_p(\mathbf{r}_p)\chi^{(-)}(\mathbf{r}_p), D_{np}S_{\mu_d}(\sigma_n,\sigma_p)\Psi_A(\theta,\xi)F_d(\mathbf{r}_d)\chi^{(+)}(\mathbf{r}_d)\rangle. \tag{4.58}$$

The functions $F_p(\mathbf{r}_p)$ and $F_d(\mathbf{r}_d)$ are given by (4.57) (the arguments γ_p and γ_d have been omitted).

The potential $V(\mathbf{r})$ in (4.57) is deformed, hence $F(\mathbf{r})$ is deformed. The modification factor $F(\mathbf{r})$ follows the nuclear contour. To first order in the deformation, the modification is

$$F(\mathbf{r})=F(r)+\beta Y_l{}^0(\hat{r}')RdF(r)dR. \tag{4.59}$$

Equation (4.19) becomes

$$T_{dp}=T_0+\beta(T_1+\delta T_1)+\cdots, \tag{4.60}$$

where δT_1 represents the added indirect contributions to the stripping reaction that are caused by the second term of Eq. (4.59).

Equations (4.20) and (4.21) for T_0 and T_1 are not altered, except for the insertion of $F_p{}^*(r_p)F_d(r_d)$ in each term. Under the zero-range approximation, this quantity has no angular dependence and is merely incorporated with the neutron form factor F_l. A modified form factor is defined by

$$\mathfrak{F}_l(r)=F_p{}^*(r)F_l(r)F_d(r). \tag{4.61}$$

The additional first-order amplitude in Eq. (4.60) is best broken into two parts:

$$\delta T_1=\delta T_p+\delta T_d, \tag{4.62}$$

where

$$\delta T_p=(N+1)^{1/2}\langle S_{\mu_p}(\sigma_p)\Psi_B(\theta,n,\xi) \times R_p[dF_p(r_p)/dR_p]Y_2{}^0(\mathbf{r}_p')\chi_0{}^{(-)}(\mathbf{r}_p), D_{np}S_{\mu_d}(\sigma_n,\sigma_p)\Psi_A(\theta,\xi)F_d(r_d)\chi_0{}^{(+)}(\mathbf{r}_d)\rangle, \tag{4.63}$$

and

$$\delta T_d=(N+1)^{1/2}\langle S_{\mu_p}(\sigma_p)\Psi_B(\theta,n,\xi)F_p(r_p)\chi_0{}^{(-)}(\mathbf{r}_p), D_{np}S_{\mu_d}(\sigma_n,\sigma_p)\Psi_A(\theta,\xi)R_d[dF_d(r_d)/dR_d] \times Y_2{}^0(\mathbf{r}_d')\chi_0{}^{(+)}(\mathbf{r}_d)\rangle. \tag{4.64}$$

These two parts can be cast in terms of the generalized single-particle transition amplitude, Eq. (4.49).

It is seen that the addition of nonlocality has little effect on the formulation of the stripping amplitude, (4.51). The changes are very slight. The form factor to be used in the generalized single-particle transition amplitude, (4.49), is $\mathfrak{F}_l(r)$, rather than $F_l(r)$. Furthermore, the differential operators d/dR_p and d/dR_d operate not only on the local optical-model wave functions, but also on the form factor $\mathfrak{F}_l(r)$. However, numerical calculations show that the derivative terms of $\mathfrak{F}_l(r)$ give rise to negligible contributions to the transition amplitude.

4.6. Differential Cross Section

The differential cross section will now be written. In the distorted-wave formulation, it is customary to define the quantity

$$\beta_{\mathrm{DWBA}}{}^{LM}=(2L+1)^{-1/2}t_L{}^{LM}. \tag{4.65}$$

The differential cross section is then cast in terms of $\beta_{\mathrm{DWBA}}{}^{LM}$. In order to maintain the formal appearance of the distorted-wave expressions, a generalized $\beta_J{}^{LM}$ is defined as[4]

$$\beta_J{}^{LM}=(2L+1)^{-1/2}[t_L{}^{LM}+\beta(C_{LJ})^{-1} \times\textstyle\sum_{lm} i^{L-l}(5/4\pi)^{1/2}\langle Lm\tfrac{1}{2}\Omega-m|J\Omega\rangle a_{lm}(\Omega) \times\langle Lm20|lm\rangle\langle l020|L0\rangle \times(R_p d/dR_p+R_d d/dR_d)t_l{}^{LM}]. \tag{4.66}$$

Then, Eq. (4.51) becomes

$$T_{dp}=g(\hat{I}_1/\hat{I}_2)\textstyle\sum_{JM_J\mu_n}\langle\frac{1}{2}\mu_n\frac{1}{2}\mu_p|1\mu_d\rangle \times\langle I_1M_1JM_J|I_2M_2\rangle\langle I_1\pm K_1J\Omega|I_2K_2\rangle \times\sum_{LM}\hat{L}\langle LM\tfrac{1}{2}\mu_n|JM_J\rangle C_{LJ}(\Omega)\beta_J{}^{LM}. \tag{4.67}$$

Assuming a random distribution of polarizations in the entrance channel, and assuming that the detector does not distinguish amongst states of different polarization in the exit channel, the differential cross section is found to be

$$d\sigma/d\Omega=g^2\textstyle\sum_J\langle I_1\pm K_1J\Omega|I_2K_2\rangle^2 \times\sum_L[C_{LJ}(\Omega)]^2\sigma_{LJ}(\beta), \tag{4.68}$$

where

$$\sigma_{LJ}(\beta)=\tfrac{1}{2}m_pm_d(2\pi\hbar^2)^{-2}(k_p/k_d)\textstyle\sum_M|\beta_J{}^{LM}|^2. \tag{4.69}$$

The quantity $[g\langle I_1\pm K_1J\Omega|I_2K_2\rangle C_{LJ}(\Omega)]^2$ is a spectroscopic coefficient, where $g\langle I_1\pm K_1J\Omega|I_2K_2\rangle$ is a measure of the overlap of the rotational wave functions, and the $C_{LJ}(\Omega)$ are the coefficients of the LJ spin-orbit functions in which the captured neutron orbital is expanded, Eq. (4.25). The quantity $\sigma_{LJ}(\beta)$ is a generalized, deformation-dependent, single-particle cross section. When β becomes zero, $\sigma_{LJ}(\beta)$ becomes the usual single-

particle cross section of distorted-wave theory.[32,33] As in the distorted-wave theory, single-particle cross sections that have different L or J simply add incoherently in the expression for the differential cross section. In other words, there is no interference between amplitudes that have different L or J. This means that if we are dealing with a stripping reaction that has strong direct contributions, we can expect that the non-normal-parity indirect contributions will have little effect, since such contributions add incoherently to the direct contributions.

5. APPLICATION TO STRIPPING ON Mg^{24} AND U^{238}

Equations (4.69) and (4.68) were coded for the University of Pittsburgh IBM 7090 computer. Input to the program consisted of distorted-wave transition amplitudes that were calculated by the code JULIE.[34] There are two indirect contributions to $\beta_J{}^{LM}$, that arise from differentiation of the distorted waves in the deuteron and proton channels. Provision was made in the code to evaluate separately the single-particle cross sections that account for each of the direct and indirect contributions. This was done in order to analyze the relative importance of each of the contributions to the stripping reaction.

Once the single-particle cross sections of Eq. (4.69) have been computed, the squares of the neutron spin-orbit coefficients, $[C_{LJ}(\Omega)]^2$, can be obtained by fitting Eq. (4.68) to the stripping data. This is especially simple for the reactions on Mg^{24} and U^{238}, because the quantum numbers L and J are known. Since these are even-even nuclei, Eq. (4.68) becomes

$$d\sigma/d\Omega=2[C_{LJ}(\Omega)]^2\sigma_{LJ}(\beta). \tag{5.1}$$

The angular momentum tranfer J must equal the spin I_2 of the product nucleus and $L=J\pm\frac{1}{2}$ is fixed by the parity of the product nucleus. Of course, the so-called "single-particle cross section" $\sigma_{LJ}(\beta)$ does have some implicit dependence on $C_{lj}(\Omega)/C_{LJ}(\Omega)$, the ratio of the indirect coefficients to the direct coefficient. The procedure adopted in this work was to use the Nilsson[11] values for the $C_{lj}(\Omega)$ in the computation of the single-particle cross sections. Of course an iterative procedure could be used instead, in that the values for $C_{LJ}(\Omega)$ obtained from experiment by Eq. (5.1) could be employed in calculating a new set of single-particle cross sections. However, an iterative procedure was used for only one case in the calculations to be discussed.

The transition amplitude calculated by the code JULIE is too small, because it uses the zero-range normalization for the deuteron wave function. The correct asymptotic amplitude of the wave function, as obtained from effective-range theory,[24] increases the single-particle cross section by a factor of 1.7. However, finite-range calculations[35] indicate some reduction of the cross section. For the present work we adopt the usual working compromise, and use a factor 1.5.

Thus, Eq. (5.1) becomes

$$d\sigma/d\Omega=3[C_{LJ}(\Omega)]^2\sigma_{LJ}{}^{(\mathrm{JULIE})}(\beta). \tag{5.2}$$

where $d\sigma/d\Omega$ is the differential cross section for stripping on an even-even nucleus, yielding a product nucleus of spin J and parity $(-1)^L$.

5.1. Stripping to the Mg^{25} Ground-State Band

The Nilsson orbit $[Nn_z\Lambda]\Omega\pi=[202]\frac{5}{2}+$ is assigned to the odd neutron of the Mg^{25} nucleus in its ground state. For this orbit the coefficient a_{lm} is unity if $l=m=2$; otherwise a_{lm} is zero. Therefore, the direct transition can excite only the $I_2=\frac{5}{2}$ ground-state level of the $K=\frac{5}{2}$ band. However, to first order in β the indirect transitions will excite the $I_2=\frac{5}{2}$, $\frac{7}{2}$, and $\frac{9}{2}$ levels of the $K=\frac{5}{2}$ band. The indirect transition amplitude is expected to be small and consequently its effects will be most pronounced when it is acting in coherence with the direct transition amplitude.

First, the transition to the ground state will be studied. Several questions are asked. (a) By how much is the differential cross section changed due to the addition of the indirect transition terms? (b) In what way does nonlocality of the optical-model potential effect these results? (c) What are the effects of changing the parameters of the deuteron optical potential? (d) What is the relative importance of the indirect contributions from excitations in the deuteron and proton channels separately?

It was assumed in the numerical calculations that the laboratory energy of the incident deuteron is 15 MeV. The optical potentials used have the standard Woods-Saxon well shape:

$$V(r)=-V_0(1+\exp x)^{-1} -i(W-W'd/dx')(1+\exp x')^{-1}. \tag{5.3}$$

The parameter x is defined by

$$x=(r-r_0A^{1/3})/a.$$

Similarly,

$$x'=(r-r_0'A^{1/3})/a'. \tag{5.4}$$

The optical parameters used in this calculation are displayed in Table I. The parameters of the shallow deuteron well are those of Melkanoff,[36] the parameters of the deep deuteron well are recommended by Bassel,[37] and the parameters of the proton well are those of

[32] W. Tobocman, *Theory of Direct Nuclear Reactions* (Oxford University Press, Oxford, 1961).
[33] R. H. Bassel, R. M. Drisko, and G. R. Satchler, Oak Ridge National Laboratory Technical Report No. ORNL-3240, 1962 (unpublished).
[34] R. M. Drisko (unpublished).
[35] N. Austern, R. M. Drisko, E. C. Halbert, and G. R. Satchler, Phys. Rev. **133**, B3 (1964).
[36] M. A. Melkanoff, F. Sawada, and N. Cindro, Phys. Letters **2**, 98 (1962).
[37] R. M. Drisko (private communication).

TABLE I. Optical-model parameters for magnesium.

	V_0(MeV)	r_0(F)	a(F)	W(MeV)	W'(MeV)	r_0'(F)	a'(F)	r_c(F)
V_d	50.0	1.50	0.59	16	0	1.500	0.59	1.50
V_d'	101.3	1.00	0.90	0	115.6	1.443	0.50	1.30
V_p	45.0	1.25	0.65	0	40.0	1.250	0.47	1.25

Johnson.[38] The binding energy of the captured neutron is determined from experiment to be $B_n=7.325$ MeV. (The code JULIE[34] utilizes the binding energy. It calculates the neutron radial functions with a Saxon well, and adjusts the well depth in order to reproduce the binding energy.) The radius of the neutron well was chosen as $1.25\ A^{1/3}$ F and the diffusivity parameter was chosen as $a=0.65$ F.

The parameters of Table I are not quite correct for the calculations. They were chosen to fit the observed elastic-scattering data. In other words, with the parameters of Table I, $\chi_0^{(+)}(\mathbf{r})$ of (3.32) fits the elastic-scattering data by itself. However, higher order terms of the expansion (3.32) contribute to the elastic scattering, and this more complete theory therefore would only be expected to fit the elastic scattering if modified parameters were used. On the other hand, the effects of the indirect contributions to the stripping cross section should not depend strongly on the precise choice of the optical-model parameters, and the parameters of Table I should be sufficient for preliminary insight.

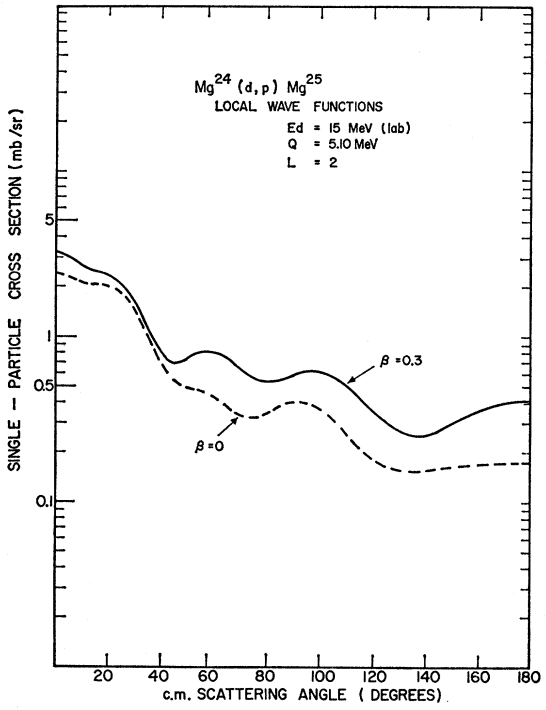

FIG. 1. Single-particle cross section for the ground-state level of Mg^{25}, for $\beta=0$, and $\beta=0.3$. Nonlocal effects are not included. The calculations were performed with the shallow deuteron well of Table I.

[38] Bibijana Čujec, Phys. Rev. **136**, B1305 (1964).

Let us turn now to the first question asked at the beginning of this section: By how much is the differential cross section altered by the addition of the indirect-transition terms? Using V_d and V_p of Table I, the differential cross section was calculated for $\beta=0$ and $\beta=0.3$. The results are displayed in Fig. 1. The two angular distributions are very similar, especially at the forward angles, where the cross sections reach their peak. The slope of the sharp drop beyond 25° is about the same for both curves. However, past 40°, the $\beta=0$ distribution shows a more prominent attenuation than does the $\beta=0.3$ distribution. In other words, the indirect amplitudes have somewhat flattened the differential cross section. This effect is expected to be quite general. The direct transition amplitude receives important contributions both from partial waves that remain outside the nucleus and from partial waves that penetrate the nuclear surface. This is because the captured neutron resides in the least-bound single-particle orbit, hence its radial wave function extends beyond the nuclear surface. However, the indirect transition amplitudes receive contributions only from those partial waves that penetrate the nuclear surface, because the perturbation that generates the indirect amplitudes is localized at the surface. Since the direct amplitude receives important contributions from higher partial waves, it experiences more phase averaging at back angles[27] amongst the differential partial waves. Hence there is a greater attenuation of the direct amplitude at back angles than of the indirect amplitude. An equivalent point of view is that angular position and angular momentum are dynamical conjugates. Because the indirect transitions are somewhat more localized in angular momentum space, they must have a broader distribution in angular-position space. In addition to these changes in shape, the $\beta=0.3$ cross section is larger than the $\beta=0$ cross section at all angles. The indirect transitions increase the cross section at the peak by a factor of about 1.3.

Let us address ourselves to the second question: In what way does nonlocality of the optical potentials effect these results? Again V_d and V_p of Table I are used, but now the neutron radial wave function is replaced by an equivalent nonlocal form factor, Eq. (4.61). The ranges of the nonlocality in the deuteron and proton channels are those found by Perey; i.e., $\gamma_d=0.54$ F and $\gamma_p=0.85$ F.[37] Unfortunately, the deuteron nonlocal range was determined for deuteron

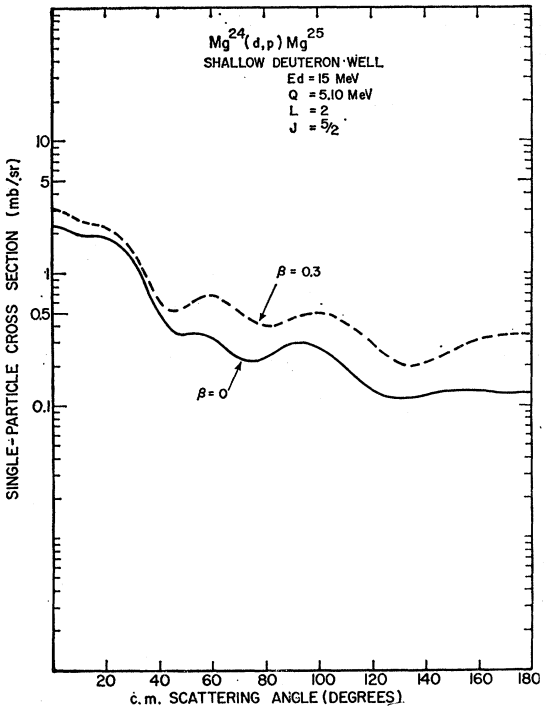

FIG. 2. Single-particle cross section for the ground-state level of Mg^{25}, for $\beta=0$, and $\beta=0.3$. Nonlocal effects are included. The calculations were performed with the shallow deuteron well of Table I.

well depths of about 100 MeV, whereas the depth of V_d is only 50 MeV. It is likely that a larger range is required for the shallow well, but no attempts were made in this direction. It should also be noted that the potential that should be used in Eq. (4.57) is the full, complex optical potential. However, only the real part of the optical potential was used in this work. Figure 2 displays the single-particle cross sections with and without deformation. The deformed cross section was calculated by including all indirect transitions; i.e., derivative terms of the scattered waves and of the equivalent nonlocal form factor were taken account of. Omitting the derivative terms of the equivalent nonlocal form factor produced a negligible change in the $\beta=0.3$ cross section. However, the differences between the angular distributions in Figs. 1 and 2 indicate that the damping of the distorted waves inside the nucleus does have a moderate effect on the angular distributions of both the $\beta=0$ and the $\beta=0.3$ differential cross sections. There is a slight decrease in the cross sections at the peak and a much larger attenuation at back angles. This seems reasonable, in that the nonlocality suppresses the low partial waves more than it suppresses the high partial waves. However, the general shapes of the curves in Figs. 1 and 2 are about the same and the effect of including the indirect transition amplitudes is unaltered. Because the nonlocality of the optical potentials has significant effects on the stripping cross section, subsequent calculations will all be done, as a matter of course, with the equivalent nonlocal form factors.

Let us turn now to the third question: What are the effects of changing the parameters of the deuteron optical potential? Replacing the shallow deuteron well of Table I with the deep deuteron well, the single-particle cross section was again calculated for $\beta=0$ and $\beta=0.3$. Although V_d' is deeper than V_d, they both are in the same $V_0r_0^2$ valley. The results are shown in Fig. 3. Again, the two angular distributions are very similar and the indirect transition amplitudes have somewhat flattened the angular distribution. And again, the $\beta=0.3$ cross section is larger than the $\beta=0$ cross section at all angles. The peak cross section is increased by a factor of 1.4. However, there are very striking differences between the differential cross section calculated with the shallow deuteron well and that calculated with the deep well. The peak cross section of the former case is almost 60% higher than that of the latter case. Furthermore, the angular distribution obtained with the deep well shows more marked oscillations and drops much more sharply from the forward peak. It is evident that the uncertainties in the magnitude and angular distribution of the single-particle cross section, due to the ambiguities in the deuteron optical-model parameters, are larger than the corrections due to the indirect transition amplitudes.

Let us turn to the question of the relative importance of the indirect transitions via excitations in each of the

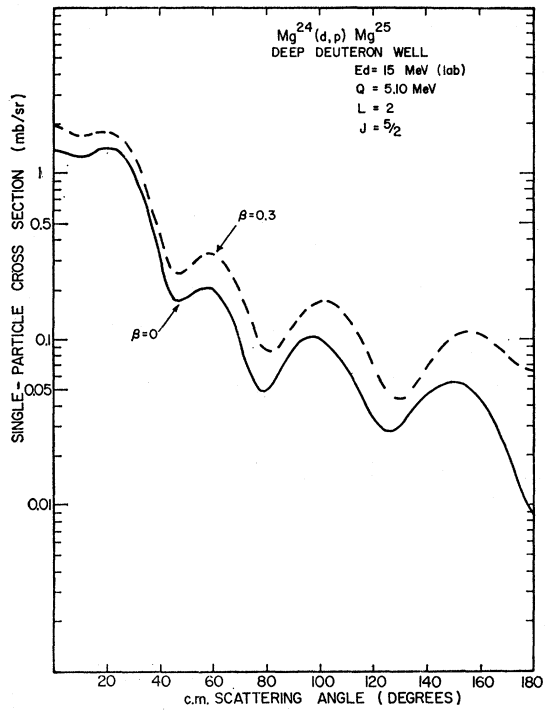

FIG. 3. Single-particle cross section for the ground-state level of Mg^{25}, for $\beta=0$ and $\beta=0.3$. The calculations were performed with the deep deuteron well of Table I.

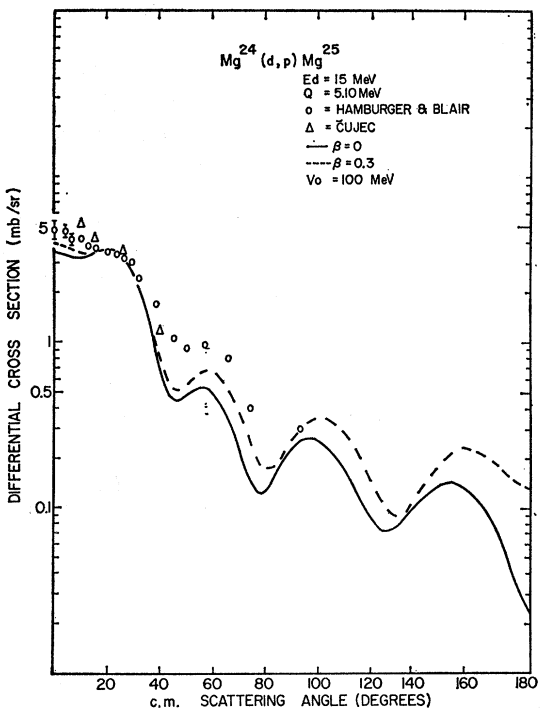

FIG. 4. Comparison of the $\beta=0$ and $\beta=0.3$ single-particle cross sections with the observed angular distribution of the transition to the ground state of Mg^{25}. The calculations were performed with the deep deuteron well of Table I.

deuteron and proton channels. In order to answer this question, the differential cross section was evaluated, allowing for indirect contributions from excitations in each of the deuteron and proton channels separately. At all angles the indirect transitions via the deuteron channel dominate those via the proton channel. When the shallow deuteron well was used, the deuteron indirect stripping amplitude was approximately three times the proton amplitude. When the deep deuteron well was used, this ratio increased to about eight or nine.

The theoretical angular distributions were compared with the data of Čujec[38] and of Hamburger and Blair.[39] The theoretical curves were calculated with the deep deuteron well. Figure 4 compares the $\beta=0$ and $\beta=0.3$ predictions with the data. The theoretical curves are normalized in order to fit the data at the shoulder at 25°. Both curves give only fair fits to the data and the $\beta=0.3$ prediction gives only a slight improvement to the fit. However, the square of the coefficient of the $L=2$, $J=\frac{5}{2}$ component of the neutron wave function, determined by Eq. (5.2) and the fits of Fig. 4, is $(C_{2,5/2})^2=0.84$ for $\beta=0$ and $(C_{2,5/2})^2=0.67$ for $\beta=0.3$. In other words, the square of the amplitude of the $L=2$, $J=\frac{5}{2}$ component of the neutron wave function is overestimated by about 25% by the $\beta=0$ prediction. The Nilsson value for this coefficient is unity; i.e., the Nilsson orbit $[202]\frac{5}{2}+$ is completely an $L=2$, $J=\frac{5}{2}$ state.

The next higher state in the ground-state band has spin $\frac{7}{2}$ and has been identified with the 1.61-MeV state. If the $[202]\frac{5}{2}+$ orbit again is adopted for the neutron wave function, then angular momentum selection rules forbid reaching this state by a direct stripping transition. However, it can be reached by an indirect transition. The differential cross section to this state was calculated, using the shallow deuteron well, and found to be about a factor of 4 smaller than the data of Hamburger and Blair. Figure 5 shows the predicted stripping cross section for the $\frac{7}{2}$ state, along with the data of Hamburger and Blair. In view of the approximate nature of the present calculation, it is not clear whether Fig. 5 should be regarded as showing agreement or disagreement between theory and experiment.

The predicted differential cross section for the $\frac{9}{2}$ state of the ground-state band is exactly 3.5 times that predicted for the spin-$\frac{7}{2}$ state. However, the $\frac{9}{2}$ state of the ground-state band has not been identified in Mg^{25}, although it has been identified in the mirror nucleus, Al^{25}.

5.2. Stripping to the Mg^{25} $K=\frac{1}{2}$ Band

The 0.58-, 0.98-, and 1.96-MeV states all are members of the $[211]\frac{1}{2}+$band, with spins $\frac{1}{2}$, $\frac{3}{2}$, and $\frac{5}{2}$, respectively. This particular Nilsson orbital has amplitudes for $L=0$ and 2 and for $J=\frac{1}{2}$, $\frac{3}{2}$, and $\frac{5}{2}$. Therefore, all three of the above states can be reached by the direct stripping process.

Because experimental cross sections are available for stripping to all three of the above states, we decided to search for the neutron wave function coefficients, C_{LJ}, which would best fit the data. Equation (5.2) was used to calculate the $(C_{LJ})^2$ from the fits of the single-particle cross sections to the experimental cross sections. An iterative procedure was used in the search. The values of the C_{LJ} calculated by Nilsson for $\beta=0.17$ were

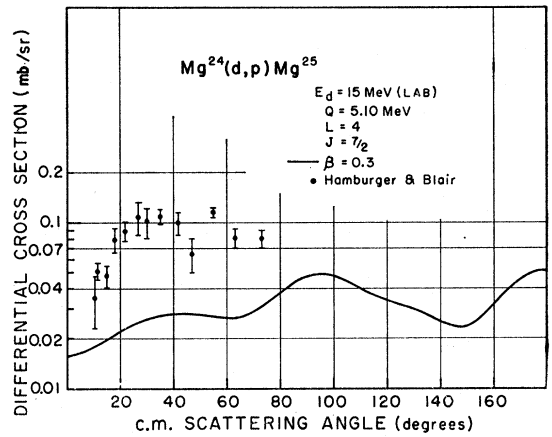

FIG. 5. Comparison of the predicted and observed, differential cross sections for the $I=\frac{7}{2}$ level in the ground-state band of Mg^{25}. The calculations were performed with the shallow deuteron well of Table I.

[39] E. W. Hamburger and A. G. Blair, Phys. Rev. 119, 777 (1960).

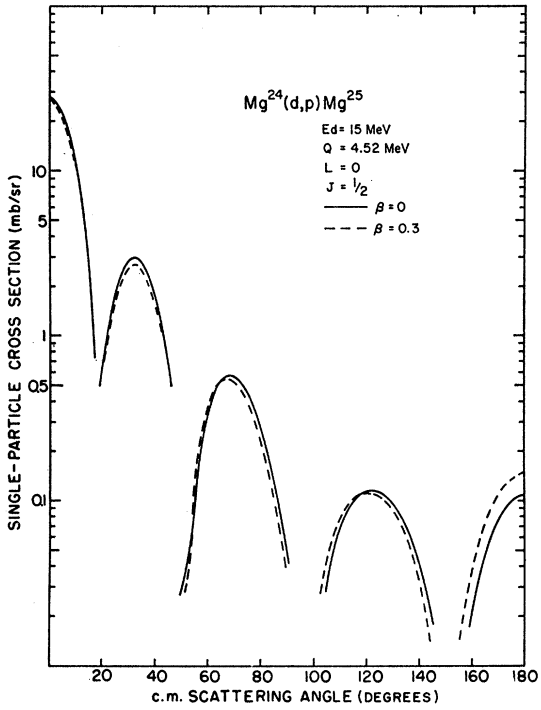

FIG. 6. Single-particle cross section for the $I=\frac{1}{2}$ level of the $[211]\frac{1}{2}+$band of Mg^{25}, for $\beta=0$ and $\beta=0.3$. These and all subsequent calculations were performed with the deep deuteron well of Table I.

used as trial values in computing the single-particle cross sections, Eq. (4.69). Through the use of Eq. (5.2), a new set of values of C_{LJ} were then calculated, and these new values were used, in turn, to compute new single-particle cross sections. This iteration procedure converged in just one iteration. Table II exhibits the starting values of the $(C_{LJ})^2$, calculated by Nilsson for $\beta=0.17$, and also exhibits the values obtained by fitting Eq. (5.2) to experiment, using both $\beta=0$ and $\beta=0.3$, for comparison. The coefficients $(C_{LJ})^2$ should sum to unity if the strong-coupling model[23] were accurate. However, both for $\beta=0$ and for $\beta=0.3$, the values of the $(C_{LJ})^2$ that are extracted from experiment sum to 1.4. The fitted values of the $(C_{LJ})^2$ were renormalized, such that the renormalized values sum to unity. These renormalized values are also shown in Table II.

The angular distributions of the $L=0$, $J=\frac{1}{2}$ single-particle cross section are displayed in Fig. 6, for $\beta=0$ and $\beta=0.3$. This cross section is hardly at all effected

TABLE II. Calculated values of the coefficients $(C_{LJ})^2$.

L	J	$\beta=0$	$\beta=0.3$	Renormalized $\beta=0$	Renormalized $\beta=0.3$	Nilsson model
0	$\frac{1}{2}$	0.54	0.58	0.40	0.41	0.20
2	$\frac{3}{2}$	0.47	0.67	0.34	0.48	0.53
2	$\frac{5}{2}$	0.36	0.16	0.26	0.11	0.27
$\Sigma(C_{LJ})^2$		1.37	1.41	1.00	1.00	1.00

TABLE III. Self-consistent, renormalized neutron orbital coefficients a_{LM} for the $[211]\frac{1}{2}+$band.

L	M	a_{LM}
0	0	0.54
2	0	0.15
2	1	−0.64

by the indirect transitions. This is easy to understand in terms of Eq. (4.50) and in terms of the expansion of the neutron orbital in the LM representation, given by

$$U_\Omega=\sum_{LM} a_{LM}\psi_{LM}S_{\frac{1}{2}\Omega-M}. \quad (4.26)$$

The states ψ_{LM} are eigenstates of the orbital angular momentum and of its projection onto the nuclear symmetry axis. The coefficients a_{LM} are related to the C_{LJ} of Eq. (4.25) by Eq. (4.27). The values of the a_{LM} that are obtained from the renormalized, iterated C_{LJ} of Table II are given in Table III. From Eq. (4.50) it is seen that only the $L=2$, $M=0$ amplitude can contribute to the indirect transition to the $L=0$, $J=\frac{1}{2}$ cross section. But this is just the smallest amplitude. Use of the Nilsson values of the a_{LM} does not alter this conclusion. The fits to the data of Čujec are shown in Fig. 7.

Figure 8 shows the angular distributions of the $L=2$, $J=\frac{3}{2}$ and $\frac{5}{2}$ transitions, for $\beta=0$ and $\beta=0.3$. The $\beta=0$ transition has no J dependence, because the optical potentials used are central. However, the angular distributions show a strong J dependence when β is non-

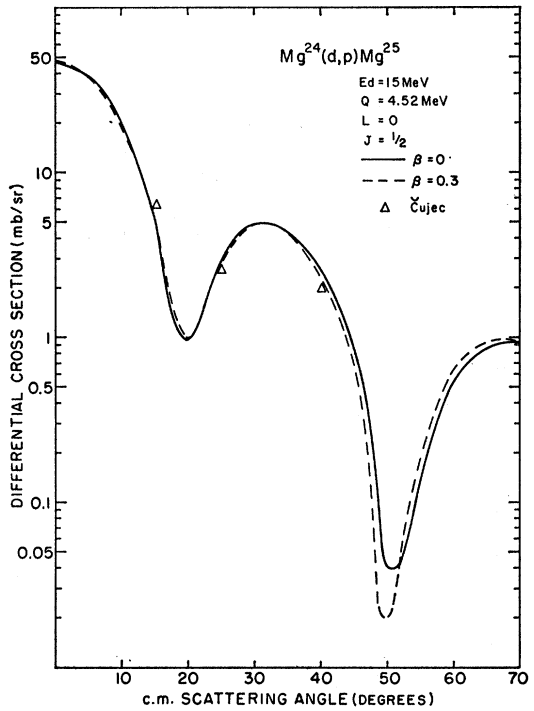

FIG. 7. Comparison of the $\beta=0$ and $\beta=0.3$ single-particle cross sections with the observed angular distribution of the transition to the $I=\frac{1}{2}$ level of the $[211]\frac{1}{2}+$band of Mg^{25}.

TABLE IV. Calculated and experimental values of the decoupling parameter, $\mathfrak{a}$.

		Renormalized		Nilsson	
$\beta=0$	$\beta=0.3$	$\beta=0$	$\beta=0.3$	model	Exp.
0.68	−0.28	0.50	−0.22	−0.05	−0.2

zero. Most noticeable is the fact that, when β is nonzero, the $J=\frac{3}{2}$ distribution flattens considerably past 70°. In general, the deformation seems to alter the $\frac{3}{2}$ and $\frac{5}{2}$ distributions in somewhat opposite directions. This can be seen to follow from the form of the J dependence of the indirect transitions, as displayed in Eq. (4.50). The entire J dependence is contained in the coefficients $\langle Lm\frac{1}{2}\Omega-m|J\Omega\rangle$. This Clebsch-Gordan coefficient has opposite signs for $J=L\pm\frac{1}{2}$ if $m=\Omega-\frac{1}{2}$, but has the same sign for $J=L\pm\frac{1}{2}$ if $m=\Omega+\frac{1}{2}$. Thus, the J dependence of the single-particle cross sections will be marked if the coefficients a_{lm} are large for $m=\Omega-\frac{1}{2}$, but will be weak if the coefficients a_{lm} are large for $m=\Omega+\frac{1}{2}$. In the case at hand the coefficients a_{lm} are so balanced as to give a partial washing out of the effect. However, for many Nilsson orbitals, the coefficients a_{lm} are unbalanced.

Figure 9 compares the $L=2$, $J=\frac{3}{2}$ predictions for $\beta=0$ and $\beta=0.3$ with the experimental results of Čujec.[38] The fit is good, but the differences between the $\beta=0$ and the $\beta=0.3$ predictions probably are too small to be significant. Figure 10 compares the $L=2$, $J=\frac{5}{2}$ predictions for $\beta=0$ and $\beta=0.3$ with the data of Hamburger and Blair[39] and of Čujec.[38] Neither prediction gives a good fit to the data insomuch as the predicted slope beyond 25° is too steep.

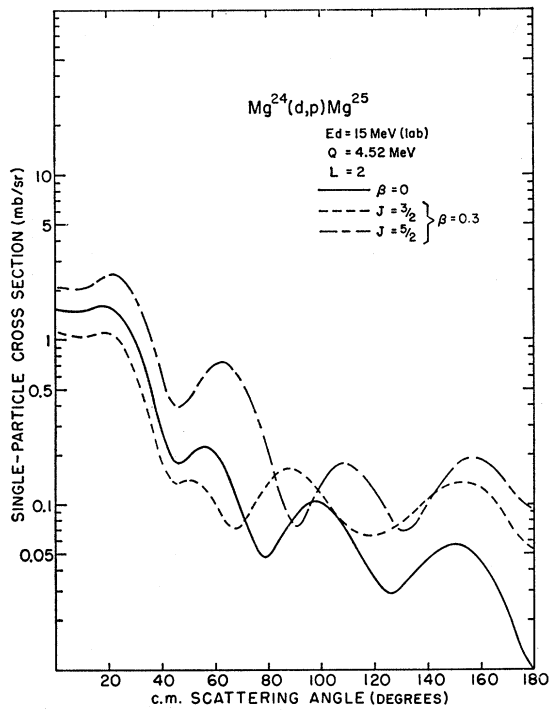

FIG. 8. Single-particle cross sections for the $I=\frac{3}{2}$ and $\frac{5}{2}$ levels of the $[211]\frac{1}{2}+$band of Mg^{25} for $\beta=0$ and $\beta=0.3$.

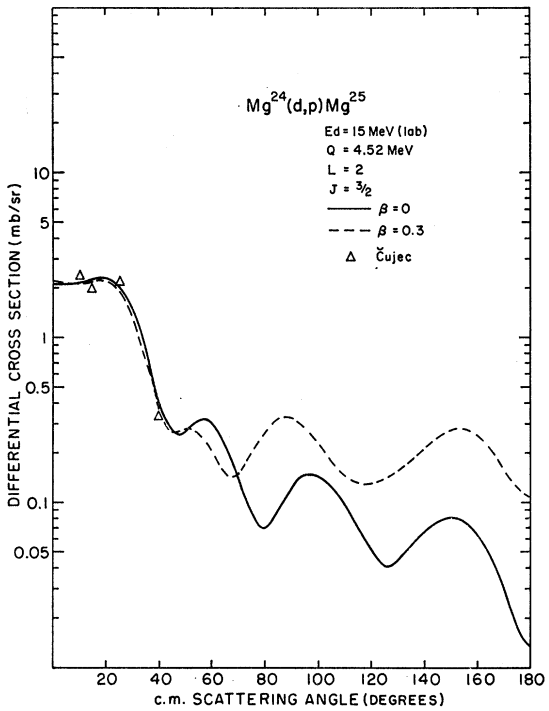

FIG. 9. Comparison between the Čujec data (see Ref. 38), and the $\beta=0$ and $\beta=0.3$ single-particle cross sections for the transition to the $I=\frac{3}{2}$ level of the $[211]\frac{1}{2}+$band of Mg^{25}.

A parameter that is sensitive to the values of the $(C_{LJ})^2$ is the decoupling parameter, $\mathfrak{a}$. Due to rotation-particle coupling, the energy spectrum of a $K=\frac{1}{2}$ band deviates from a pure rotational spectrum. The energy spectrum is

$$E(I)=E_0+(\hbar^2/2\mathcal{I})[I(I+1)+(-1)^{I+\frac{1}{2}}(I+\tfrac{1}{2})\mathfrak{a}], \quad (5.3)$$

where $\mathcal{I}$ is the moment of inertia of the nucleus, I is the nuclear spin, and $\mathfrak{a}$ is the decoupling parameter. Observations of the energy levels of Mg^{25} indicate that $\mathfrak{a}$ is about -0.2. However, the decoupling parameter is given by

$$\mathfrak{a}=\sum_J(-1)^{J-\frac{1}{2}}(J+\tfrac{1}{2})|C_J|^2, \quad (5.4)$$

where the C_J are the coefficients in the expansion of the intrinsic wavefunction in eigenfunctions of the total intrinsic angular momentum. In the extreme single-particle model of deformed nuclei, all orbitals of Mg^{25} are paired except the $[211]\frac{1}{2}+$orbital. Therefore, the coefficients $|C_J|^2$ in Eq. (5.4) are just the coefficients $(C_{LJ})^2$ of the $[211]\frac{1}{2}+$orbital. Equation (5.4) was used to calculate the decoupling parameter by substituting $(C_{LJ})^2$ for $|C_J|^2$. The values of $(C_{LJ})^2$ were taken from Table II. The results are given in Table IV. The experimental value of $\mathfrak{a}$ favors the $\beta=0.3$ results over the $\beta=0$ results. However, the excellent agreement between the $\beta=0.3$ value of the decoupling parameter and the

TABLE V. Optical-model parameters for uranium.

	V_0(MeV)	r_0(F)	a(F)	W(MeV)	W'(MeV)	r_0'(F)	a'(F)	r_c(F)
V_d	106.0	1.12	0.91	0	52.8	1.38	0.75	1.30
V_p	65.3	1.25	0.65	0	46.0	1.25	0.76	1.25

experimental value should be regarded as fortuitous in view of the poor fit of the $L=2$, $J=\frac{5}{2}$ single-particle cross section to the data. It is interesting that the values of the $(C_{LJ})^2$ that we find from experiment, using $\beta=0.3$, strongly resemble the values calculated by Bishop[40] for the purpose of fitting the value of $\mathfrak{A}$.

5.3. Stripping on U^{238}

It seemed desirable to do a calculation for a heavy target. Accurate stripping data for heavy nuclei are scarce. Macefield and Middleton[40] recently published data for deuteron stripping on U^{238} and compared the data to distorted-wave predictions. Because their accurate data had been made available, it was decided to treat deuteron stripping on U^{238}.

Measurements of the intrinsic quadrupole moments of nuclei in the actinide region indicate a deformation of about[41] 0.25. The ground state of Pu^{241} has been identified with the $[622]\frac{5}{2}+$orbital for the odd neutron.[41,42] Since Pu^{241} differs from U^{239} only by two proton orbitals, the odd neutron in U^{239} ought to also occupy the $[622]\frac{5}{2}+$orbital in the U^{239} ground state. This assignment is consistent with the beta decay[42] of U^{239}.

The experiment reported by Macefield and Middleton was performed with a deuteron energy of 12 MeV. The binding energy of the captured neutron in the U^{239} ground state is 4.8 MeV, and this was the value used for the binding energy of the neutron orbital in the code JULIE.[34] The optical-model parameters used were those recommended by Bassel[37] and they are listed in Table V. Table VI shows Nilsson amplitudes C_{LJ} for the $[622]\frac{5}{2}+$orbital, for a deformation of $\beta=0.25$. This table also shows computed energies of excitation for the various corresponding levels of the ground-state band of U^{239}. These energies were computed by assuming that the spin-$\frac{7}{2}$ state appears at 40 keV, the same energy at which it was located[43] in Pu^{241}.

TABLE VI. Neutron orbital coefficients C_{LJ} assumed for the $[622]\frac{5}{2}+$band.

L	J	C_{LJ}	E_x(keV)
2	5/2	−0.237	0
4	7/2	−0.002	40
4	9/2	−0.804	92
6	11/2	−0.488	155
6	13/2	0.245	230

[40] G. R. Bishop, Nucl. Phys. **14**, 376 (1959).
[41] B. E. F. Macefield and R. Middleton, Nucl. Phys. **59**, 561 (1964).
[42] Ben R. Mottelson and Sven Gösta Nilsson, Kgl. Danske Videnskab. Selskab, Mat. Fys. Skrifter **1**, No. 8 (1959).
[43] R. C. Helon, Phys. Rev. **104**, 1466 (1956).

The single-particle cross sections were calculated for the $L=2$ and $L=4$ transitions, both for $\beta=0$ and $\beta=0.25$. The $L=2$ single-particle cross sections are shown in Fig. 11. The $\beta=0.25$ angular distribution is considerably flattened with respect to the $\beta=0$ distribution. Figure 12 shows the corresponding fits to the data of Macefield and Middleton. Unfortunately, the $\beta=0$ fit is better than the $\beta=0.25$ fit.

Figure 13 shows the $L=4$, $J=\frac{9}{2}$ fits to the data of Macefield and Middleton for both $\beta=0$ and $\beta=0.25$. The $\beta=0.25$ prediction differs very little from the $\beta=0$ prediction. Both curves fit the data beyond 55° but overestimate the cross section below 55°.

Because its direct component is tiny, the $L=4$, $J=\frac{7}{2}$ cross section for $\beta=0.25$ is almost entirely indirect. The predicted differential cross section is shown in Fig. 14. The cross section is small and this is consistent with the fact that the transition was not observed.

Again, Eq. (5.2) was used in order to extract $(C_{LJ})^2$ from the data. Since only transitions to the ground state and the 92-keV excited state ($J=\frac{9}{2}$) were observed,

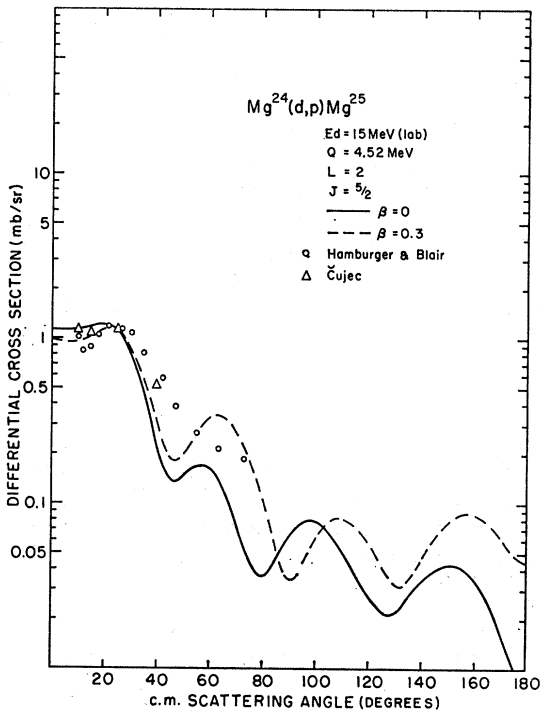

FIG. 10. Comparison between the Čujec data (see Ref. 38), the Hamburger and Blair data (see Ref. 39), and the $\beta=0$ and $\beta=0.3$ single-particle cross sections for the transition to the $I=\frac{5}{2}$ level of the $[211]\frac{1}{2}+$band of Mg^{25}.

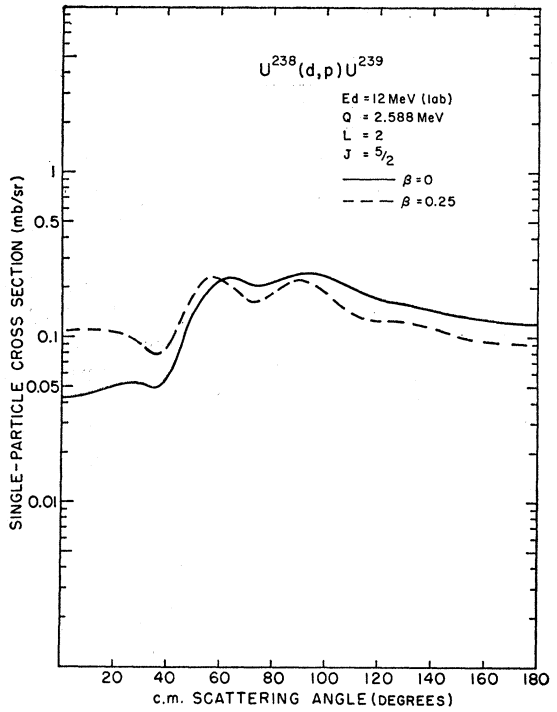

FIG. 11. Single-particle cross sections for the ground state of U^{239} for $\beta=0$ and $\beta=0.25$.

$(C_{LJ})^2$ can be calculated for only $L=2$, $J=\frac{5}{2}$ and $L=4$, $J=\frac{9}{2}$. The results are shown in Table VII.

The $\beta=0.25$ results are little different from the $\beta=0$ results. This is a reflection of the fact that the corresponding single-particle cross sections for $\beta=0$ and $\beta=0.25$ are similar in magnitude. The reason for this is that the individual indirect amplitudes, although of significant magnitude, interfere destructively. For instance, the orbital angular momentum transfer is $L=2$ for the transition to the U^{239} ground state. However, the indirect transitions can proceed by a neutron orbital angular momentum transfer of $l=2$ or $l=4$. It just so happens that the $l=2$ and $l=4$ indirect transitions have very nearly opposite phases.

5.4. Comparison of U^{238} with Mg^{24}

In comparing the magnesium and uranium cases it is desirable to distinguish the specifically size-dependent effects of the deformation from those differences which arise from the fact that the neutron orbitals are different. The angle-dependent part of the stripping amplitude is

$$\hat{L}\beta_J{}^{LM}=t_L{}^{LM}+\beta\sum_{LM}\langle Lm\tfrac{1}{2}\Omega-m|J\Omega\rangle \times i^{L-l}(5/4\pi)^{1/2}(a_{lm}/C_{LJ})\langle Lm20|lm\rangle\langle l020|L0\rangle \times(R_d d/dR_d+R_p d/dR_p)t_l{}^{LM}. \quad (4.66)$$

The amplitude $t_L{}^{LM}$ is just the undeformed amplitude. The influence of the dynamics of the neutron orbital is contained in the amplitude a_{lm} and in the associated vector-coupling coefficients, whereas the influence of the dynamics of the scattered particles is contained wholly within the factor $(R_d d/dR_d+R_p d/dR_p)t_l{}^{LM}$. We are interested in the relative size of the indirect to the direct transition amplitude, therefore, let us concentrate our attention on the dynamical ratio $|(R_d d/dR_d+R_p d/dR_p)t_l{}^{LM}|/|t_L{}^{LM}|$. It is then this ratio that is a measure of the effects of the deformation on the scattered waves in the deuteron and proton channels; therefore, it is just this ratio that contains the specifically size-dependent effects that are caused by including the indirect transitions in the calculation of the stripping cross section.

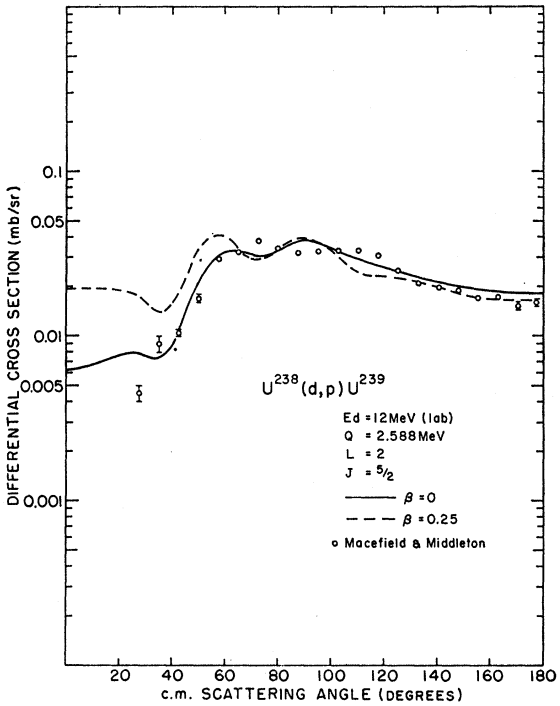

FIG. 12. Comparison of the $\beta=0$ and $\beta=0.25$ single-particle cross sections with the observed angular distribution of the transition to the ground state of U^{239}.

On the average, this dynamical ratio is about the same for both the magnesium and the uranium targets. This fact may be at least qualitatively understood in terms of the penetration of the distorted waves into the nuclear interior. In the uranium case, the Coulomb barrier is considerably higher than it is for the magnesium case; thus there is relatively more reflection of the scattered projectiles from the region outside of the

TABLE VII. Calculated values of the coefficients $(C_{LJ})^2$.

L	J	$\beta=0$	$\beta=0.25$
2	5/2	0.049	0.058
4	9/2	0.89	1.02

nucleus. On the other hand, the projectiles that scatter on the magnesium target experience relatively more transmission into the nuclear interior. Now, that portion of the scattering wave function that penetrates into the nuclear interior is highly sensitive to the nuclear radius, whereas that portion that is reflected from the Coulomb barrier is relatively insensitive to the nuclear radius. Therefore, it is to be expected that $(d/dR)t_l^{LM}$ will be smaller in the uranium case than in the magnesium case. However, the increase in the nuclear radius seems to be just about sufficient to offset this decrease, and the net effect is that the dynamical ratio is unchanged. However, we must bear in mind that the laboratory energy of the deuteron projectile was 15 MeV for the magnesium case and only 12 MeV for the uranium case. The lower energy of the incident deuteron for the uranium case undoubtedly contributed to the lack of penetration of the scattered waves. Therefore, we should expect larger contributions from the indirect

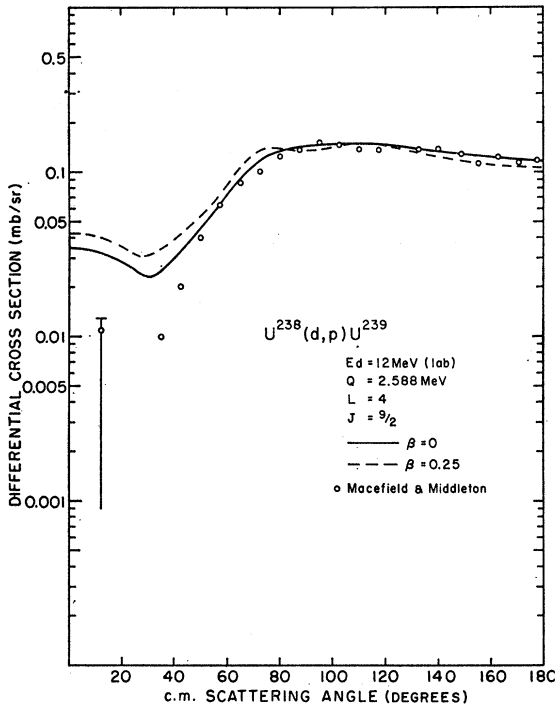

FIG. 13. Comparison of the $\beta=0$ and $\beta=0.25$ single-particle cross sections to the observed angular distribution of the transition to the $I=\frac{9}{2}$ level of the ground-state band of U^{239}.

transitions as the energy of the deuteron beam increases. Probably as the energy would rise still further, the stripping amplitude would begin to depend less upon the form of the nuclear attraction, and the contributions of the indirect transitions would again decrease.

6. DISCUSSION

A formulation has been developed for handling the corrections to the direct stripping process in deformed nuclei that are due to inelastic coupling in both deuteron and proton channels. The coupling of the elastic channels with the inelastic channels has been treated only to first order. The calculation can be viewed as a sum of three diagrams. In Fig. 15 the three amplitudes are displayed in their order of importance. In those cases where it is not inhibited by selection rules, the direct amplitude makes the major contributions to the differential cross section.

The most prominent effect of the indirect amplitudes is the flattening of the angular distributions at large angles. This is especially interesting in view of the distorted-wave analysis of the magnesium data of Middleton and Hinds[44] by Buck and Hodgson.[45] In that case the measured distributions are consistently flatter than the calculated distributions.

The contributions of the indirect transitions are remarkably independent of the atomic number of the target. This seems to result from a balancing of two competing influences. The magnitude of the inelastic perturbation is proportional to the radius of the target. This alone would cause the indirect amplitudes to increase with A. On the other hand, there is more reflection from the Coulomb field of a heavy nucleus, thereby reducing the overlap of the inelastic perturbation with the zero-order wave function.

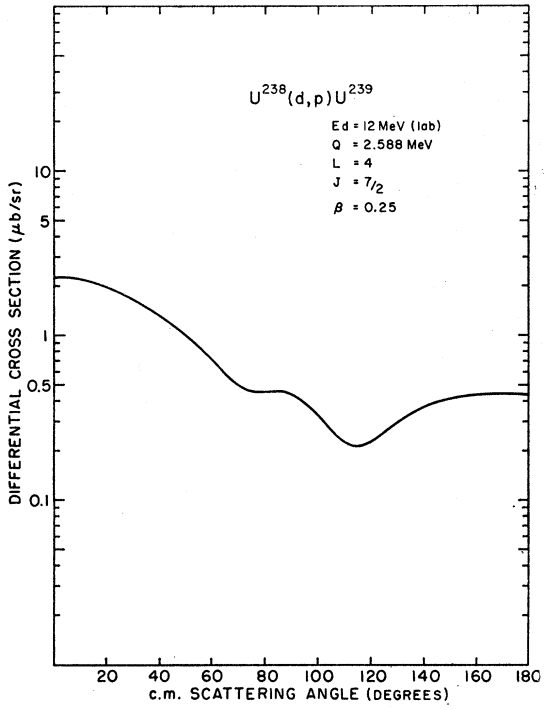

FIG. 14. Predicted differential cross section for the $I=\frac{7}{2}$ level of the ground-state band of U^{239}, for $\beta=0.25$.

[44] R. Middleton and S. Hinds, Nucl. Phys. 34, 404 (1962).
[45] B. Buck and P. E. Hodgson, Nucl. Phys. 29, 496 (1962).

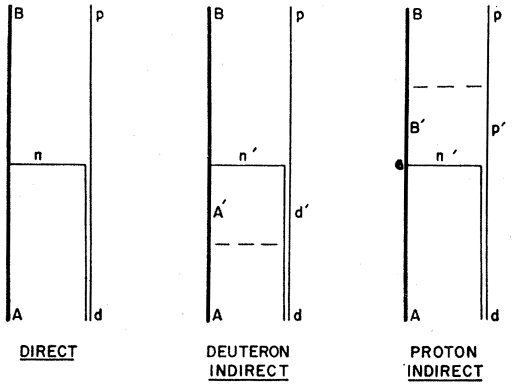

FIG. 15. The three terms in the transition amplitude of the reaction $A(d,p)B$ that are computed in this work. The solid lines represent the particles and the dashed lines represent the inelastic-scattering interactions.

It was suggested by de-Shalit[46] that the interaction that generates the indirect amplitude need not have a $dV_0(r)/dR$ form, where $V_0(r)$ is the optical potential. Instead, this interaction may reside beyond the range of the optical potential. This could change the complexion of the penetrability arguments given in the last paragraph. An interaction that lies outside of the nuclear surface may produce larger effects in heavy nuclei than in light nuclei. There is evidence for a small systematic effect of this kind in the inelastic scattering of deuterons and protons. Increasing the range of the interaction that is responsible for inelastic scattering might also moderate the flattening of the angular distribution by the indirect contribution.

The indirect contributions, to the single-particle cross section, from the deuteron channel were compared with those from the proton channel for the transition to the Mg^{25} ground state. The contributions from the deuteron channel dominated the indirect amplitudes, and this effect was especially pronounced with the deep deuteron optical potential. Using the methods of Austern and Blair,[26] the transition amplitude for inelastic scattering can easily be computed up to first order in β. The inelastic amplitudes in the deuteron and proton channels were computed for the magnesium target, using for the optical potential parameters the proton well and the deep deuteron well of Table I. On the average, the inelastic transition amplitude in the proton channel is almost five times that in the deuteron channel. These results indicate that the features of the inelastic wave function that determine the two-step stripping amplitude are different from those features that determine the inelastic-scattering amplitude.

The indirect amplitudes impose a J dependence on the angular distribution. The J dependence in the magnesium calculation, Fig. 8, is especially strong at back angles. This is reasonable, since the direct amplitude is small at these angles. It seems unlikely that this J dependence could show the smooth dependence on mass number that was found in recent work by Lee and Schiffer.[47]

In view of the approximate nature of the calculation, it should be regarded primarily as an orientation to the effects caused by coupling the projectile motion to the rotational motion of the target nucleus. Large ambiguities in the parameters of the deuteron optical potential lead to sizeable uncertainties in the zero-order transition amplitude. And, since the indirect transition via the deuteron channel dominates the first-order amplitude, there are also large uncertainties in the first-order transition amplitude. Calculations have been performed that test the sensitivity of the single-particle cross sections to the deuteron optical-model parameters. They indicate that the numerical computations, presented in Sec. 5, are rather sensitive to reasonable changes in the deuteron optical-model parameters. However, the gross features of the effects of the indirect transitions are reasonably independent of the deuteron optical-model parameters.

ACKNOWLEDGMENTS

We would like to acknowledge many helpful conversations with Dr. Richard M. Drisko and we are grateful to him for the use of his distorted-wave code, JULIE. We would like to thank Frank Rybicki for his assistance with the numerical calculations.

In performing the calculations reported in this paper, use was made of the University of Pittsburgh Computer Center, supported in part by the National Science Foundation under Grant No. G-11309.

[46] A. de-Shalit, in Proceedings of the 1965 Brookhaven Summer Study Group, edited by J. Weneser and E. Warburton, (unpublished).

[47] L. L. Lee, Jr., and J. P. Schiffer, Phys. Rev. **136**, B405 (1964).